Transcriptome profiling of lumpfish (Cyclopterus lumpus) head kidney to Renibacterium salmoninarum at early and chronic infection stages

Hajarooba Gnanagobal, Setu Chakraborty, Ignacio Vasquez, Joy Chukwu-Osazuwa, Trung Cao, Ahmed Hossain, My Dang, Katherine Valderrama, Surendra Kumar, Gabriela Bindea, et al.

Developmental and Comparative Immunology 156 (2024) 105165

Contents lists available at ScienceDirect

Developmental and Comparative Immunology

journal homepage: www.elsevier.com/locate/devcompimm

Transcriptome profiling of lumpfish (*Cyclopterus lumpus*) head kidney to *Renibacterium salmoninarum* at early and chronic infection stages

Hajarooba Gnanagobal [a,*], Setu Chakraborty [a], Ignacio Vasquez [a], Joy Chukwu-Osazuwa [a], Trung Cao [a], Ahmed Hossain [a], My Dang [a], Katherine Valderrama [a], Surendra Kumar [a,b], Gabriela Bindea [c,d,e], Stephen Hill [f], Danny Boyce [g], Jennifer R. Hall [h], Javier Santander [a,**]

[a] Marine Microbial Pathogenesis and Vaccinology Laboratory, Department of Ocean Sciences, Memorial University of Newfoundland, St. John's, NL, Canada
[b] Ocean Frontier Institute, Ocean Sciences Centre, Memorial University of Newfoundland, St. John's, NL, Canada
[c] INSERM, Laboratory of Integrative Cancer Immunology, 75006, Paris, France
[d] Equipe Labellisée Ligue Contre Le Cancer, 75013, Paris, France
[e] Centre de Recherche des Cordeliers, Sorbonne Université, Université de Paris, 75006, Paris, France
[f] Cold-Ocean Deep-Sea Research Facility, Department of Ocean Sciences, Memorial University of Newfoundland, St. John's, NL, A1C 5S7, Canada
[g] The Dr. Joe Brown Aquatic Research Building (JBARB), Ocean Sciences Centre, Memorial University of Newfoundland, St. John's, NL, Canada
[h] Aquatic Research Cluster, CREAIT Network, Ocean Sciences Centre, Memorial University of Newfoundland, St. John's, NL, Canada

ARTICLE INFO

Keywords:
Bacterial kidney disease
Renibacterium salmoninarum
Immune suppressive pathogen
Lumpfish
RNA sequencing

ABSTRACT

Renibacterium salmoninarum causes Bacterial Kidney Disease (BKD) in several fish species. Atlantic lumpfish, a cleaner fish, is susceptible to *R. salmoninarum*. To profile the transcriptome response of lumpfish to *R. salmoninarum* at early and chronic infection stages, fish were intraperitoneally injected with either a high dose of *R. salmoninarum* (1×10^9 cells dose^{-1}) or PBS (control). Head kidney tissue samples were collected at 28- and 98-days post-infection (dpi) for RNA sequencing. Transcriptomic profiling identified 1971 and 139 differentially expressed genes (DEGs) in infected compared with control samples at 28 and 98 dpi, respectively. At 28 dpi, *R. salmoninarum*-induced genes ($n = 434$) mainly involved in innate and adaptive immune response-related pathways, whereas *R. salmoninarum*-suppressed genes ($n = 1537$) were largely connected to amino acid metabolism and cellular processes. Cell-mediated immunity-related genes showed dysregulation at 98 dpi. Several immune-signalling pathways were dysregulated in response to *R. salmoninarum*, including apoptosis, alternative complement, JAK-STAT signalling, and MHC-I dependent pathways. In summary, *R. salmoninarum* causes immune suppression at early infection, whereas lumpfish induce a cell-mediated immune response at chronic infection. This study provides a complete depiction of diverse immune mechanisms dysregulated by *R. salmoninarum* in lumpfish and opens new avenues to develop immune prophylactic tools to prevent BKD.

1. Introduction

Lumpfish (*Cyclopterus lumpus*), a native fish from the North Atlantic, is utilized as an eco-friendly cold-water cleaner fish (i.e., living pest remover) to manage sea lice infestations (Imsland et al., 2014; Powell et al., 2018). Due to its endurance in cold water, lumpfish are favored over wrasses (*Labridae* spp.) for biological delousing in Atlantic salmon (*Salmo salar*) farms (Imsland et al., 2014). In small Atlantic salmon sea pens, lumpfish lice removal efficacy was reported as 93–97% (Imsland et al., 2018). In a two-year study of Norwegian commercial Atlantic salmon net pens, lumpfish with sea lice in their stomach ranged from 0 to 47%, and the cleaning efficacy (average number of ingested sea lice per lumpfish) varied from 0 to 120 with an average of 0.6 (Boissonnot et al., 2022). According to Imsland et al. (2018), lumpfish had the greatest efficacy at removing pre-adult and adult lice when stocked at 8% stocking density (Imsland et al., 2018). Like all fish species, lumpfish

* Corresponding author. Memorial University of Newfoundland, Department of Ocean Sciences, Marine Microbial Pathogenesis and Vaccinology Laboratory, 0 Marine Lab Rd, Logy Bay, NL, A1C 5S7, Canada.
** Corresponding author. Memorial University of Newfoundland, Department of Ocean Sciences, Marine Microbial Pathogenesis and Vaccinology Laboratory, 0 Marine Lab Rd, Logy Bay, NL, A1C 5S7, Canada.
E-mail addresses: hgnanagobal@mun.ca (H. Gnanagobal), jsantander@mun.ca (J. Santander).

https://doi.org/10.1016/j.dci.2024.105165
Received 28 September 2023; Received in revised form 8 March 2024; Accepted 15 March 2024
Available online 16 March 2024

encounter health challenges, and bacterial infections are the most common (Powell et al., 2018).

R. salmoninarum is a Gram-positive, non-motile, facultative intracellular pathogen that causes Bacterial Kidney Disease (BKD) in wild and cultured salmonids in fresh and marine waters across North America, South America, Europe, and Asia (Sanders and Fryer, 1980; Wiens, 2011). *R. salmoninarum* is more persistent in fish populations because of its ability for horizontal and vertical transmission (Evelyn, 1993). *R. salmoninarum* has also been found in non-salmonids, including ayu (*Plecoglossus altivelis*), North Pacific hake (*Merluccius productus*), sablefish (*Anoplopoma fimbria*), Pacific herring (*Clupea pallasii pallasii*), sea lamprey (*Petromyzon marinus*) as well as bivalve molluscs (Byford et al., 2020; Eissa et al., 2006; Gnanagobal and Santander, 2022; Pascho et al., 2002). While outbreaks of Gram-positive pathogens have not been documented in lumpfish, *R. salmoninarum* has recently been identified as a pathogen that affects this species (Gnanagobal et al., 2021). Lumpfish showed susceptibility to *R. salmoninarum,* and fish infected with a high dose (10^9 cells per fish) showed 35% mortality and characteristic clinical signs of BKD (Gnanagobal et al., 2021). Since lumpfish is an emerging aquaculture species, sufficient knowledge of its susceptibility and biology, including immune responses or functions, is still lacking (Brooker et al., 2018; Powell et al., 2018; Rønneseth et al., 2017).

The teleost immune system is highly diverse but physiologically similar to that of higher vertebrates and employs both innate and adaptive immunity (Eggestøl et al., 2018; Uribe et al., 2011). Functional analyses of some lumpfish immune mechanisms, immune cells, and effector molecules have been reported (Haugland et al., 2012; Rønneseth et al., 2015). For instance, innate immune processes such as phagocytosis and respiratory burst have been demonstrated to be functional in lumpfish (Haugland et al., 2012). Additionally, Rønneseth et al. (2015) reported the phagocytic propensity of IgM^+ B cells, suggesting a crucial role for phagocytic B cells in lumpfish innate immunity (Rønneseth et al., 2015). Moreover, lumpfish is able to produce specific antibodies upon immunization, proving the species' adaptive immunity (Rønneseth et al., 2015). Previous studies have also revealed lumpfish immune responses to bacterial infections (Dang et al., 2021; Gnanagobal et al., 2021). Canonical immune genes related to cytokines (i.e., *il8b*, *il10*, and *ifng*), chemokines (i.e., *ccl19*, *ccl20*), humoral (i.e., *igha*, *ighb*), and adaptive (i.e., *cd8a*, *cd74*) immunity were subtly stimulated in lumpfish larvae in response to oral immunization with bio-encapsulated *V. anguillarum* bacterin through live feed, *Artemia salina* (Dang et al., 2021). Moreover, lumpfish was significantly upregulated the cell-mediated adaptive immunity (i.e., *cd74*) in response to *R. salmoninarum* during the chronic infection (Gnanagobal et al., 2021).

RNA sequencing (RNA-seq) based fish transcriptomics utilizes high-throughput sequencing methods to provide insights on host-pathogen interactions during the course of infection (Kukurba and Montgomery, 2015; Sudhagar et al., 2018). Understanding the disease and developing effective immune prophylactic measures requires a thorough knowledge of how the host and the pathogen interact (Gnanagobal and Santander, 2022). The RNA-seq research on fish immune responses to pathogens not only reveals the host-immune strategies that are triggered against the pathogen but also explains how the pathogen circumvents the host-mediated defense (Sudhagar et al., 2018). An RNA-seq-based *de novo* transcriptomics study has characterized the early innate immune responses of lumpfish head kidney leucocytes following *in vitro* exposure to *V. anguillarum* O1 at 6 and 24 h post-exposure (Eggestøl et al., 2018). The complement system and TLR signalling pathway were shown to be the most highly upregulated innate immune responses in lumpfish, and according to differential expression analysis, highly upregulated cytokines were *il1b*, *il6*, *il8*, and *tnfa*. We have already used qPCR to study the immune response of lumpfish to *R. salmoninarum* infection in the head kidney at 28 and 98 days post-infection (dpi) and examined the differential expression of 33 immune-relevant transcripts (Gnanagobal et al., 2021). However, profiling the head kidney transcriptome of lumpfish using RNA-seq would be valuable to further our knowledge of host-pathogen interactions between lumpfish and the Gram-positive *R. salmoninarum* and to depict a comprehensive picture of the fish host's immune pathways involved.

There is a moderate risk of disease transfer from lumpfish to salmon or vice versa during cohabitation as the cleaner fish industry grows and the number of lumpfish interacting closely with salmon rises (Rimstad et al., 2017). Also, lumpfish with a potential pathogen load could serve as an asymptomatic vector and spread disease to the cohabitating salmon (Brooker et al., 2018; Gnanagobal et al., 2021). *R. salmoninarum* primarily infects salmonids, and the Atlantic salmon head kidney transcriptome response against live and dead *R. salmoninarum* has been reported using microarray analyses (Eslamloo et al., 2020a, 2020b; Wiens, 2011). In contrast, the lumpfish transcriptome response to a Gram-positive pathogen like *R. salmoninarum* has yet to be documented. Therefore, in the present study, we profiled the lumpfish head kidney transcriptome response to *R. salmoninarum* at early (28 dpi) and chronic (98 dpi) infection stages using reference genome-guided RNA-seq analyses. We aimed to identify and compare the immune pathways differentially regulated in response to *R. salmoninarum* at 28 and 98 dpi, thus developing a better understanding of the genes and the molecular mechanisms associated with the lumpfish response to this pathogen. In addition, to understand the innate and adaptive immunity-related immune functions in lumpfish upon *R. salmoninarum* infection, we examined lysozyme activity and *R. salmoninarum* specific antibody titers in lumpfish serum at 14, 28, 42, 56, and 98 dpi. Overall, the findings of our study provide insights into lumpfish immunity against a Gram-positive pathogen and may serve as baseline knowledge to understand the host-pathogen interactions between lumpfish and *R. salmoninarum*.

2. Materials and methods

2.1. Renibacterium salmoninarum culture

R. salmoninarum (type strain ATCC 33209) was cultured in 1 L of KDM-2 (1.0% peptone (Difco), 0.05% yeast (Difco), 0.05% L-cysteine HCl (Sigma-Aldrich, St. Louis, MO, USA), 10% fetal bovine serum (Gibco, Thermofisher, Waltham, CA, USA), 1.5% *R. salmoninarum* conditioned metabolite) (Evelyn et al., 1990) at 15 °C with aeration at 180 rpm for 10–15 days. Bacterial inoculum for infection was prepared and enumerated as previously described (Gnanagobal et al., 2021). Briefly, *R. salmoninarum* cells grown in KDM-2 were harvested at optical density (O.D. 600 nm) of 0.8 ($\sim 1 \times 10^8$ CFU mL^{-1}) and washed with phosphate-buffered saline (PBS, pH 7.0; 136 mM NaCl, 2.7 mM KCl, 10.1 mM Na_2HPO_4, 1.5 mM KH_2PO_4) (Sambrook and Russel, 2001) by centrifugation (6000 rpm for 10 min at 4 °C). The bacterial pellet was then resuspended in PBS. Bacterial cells in suspension were quantified using flow cytometry and bacteria counting kit (Invitrogen, Thermofisher Scientific, Eugene, OR, USA) according to the manufacturers' instructions. The final dose for infection was prepared to have a concentration of 1×10^9 cells $dose^{-1}$. We used a relatively high dose to ensure mortalities and strong lumpfish immune response to *R. salmoninarum* (Gnanagobal et al., 2021).

2.2. Lumpfish

Lumpfish were cultured and maintained at the Joe Brown Aquatic Research Building (JBARB; Ocean Sciences Centre, St. John's, NL, Canada). Lumpfish infection assays were carried out in the aquatic level 3 (AQ3) biocontainment unit at the Cold-Ocean Deep-Sea Research Facility (CDRF; Ocean Sciences Centre, St. John's, NL, Canada) conducted under protocols #18-01-JS, #18-03-JS, and biohazard license L-01. This study was conducted in compliance with the ARRIVE guidelines (https://arriveguidelines.org). All animal-related procedures in this study were examined and approved by the Memorial University of Newfoundland's (MUN) (https://www.mun.ca/research/about/acs/acc/) Institutional Animal Care Committee and the Biosafety

Committee in accordance with the guidelines of the Canadian Council on Animal Care (https://ccac.ca/).

Two weeks prior to infection, fish were transferred to 500 L tanks (60 fish per tank at a biomass of 25 kg m^{-3}) supplied with filtered and UV-treated seawater (33 ppt) at flow-through of 7.5 L min^{-1} and 95–110% air saturation, for acclimation at 8–10 °C. Fish were fed at 0.5% of their average body weight daily using commercial dry pellets (Skretting - Europa 15; 3–4 mm) and kept under 12 h light: 12 h dark photoperiod during the adaptation and the experimental period.

2.3. Infection and sampling

Lumpfish fasted for 24 h before injection and sampling. Each fish was intraperitoneally (i.p.) injected with either 100 µl of 10^9 cells $dose^{-1}$ *R. salmoninarum* (infected group) or 100 µl of PBS (control group) (Fig. 1A). Mortalities were recorded daily in the duplicate lumpfish group i. p., injected with the high dose. Mortalities started at 20 dpi, gradually increased, and remained steady after 50 dpi (Gnanagobal et al., 2021). The cumulative mortality at 98 dpi was 35% (Fig. 1B). Considering the mortality (Fig. 1B) and head kidney colonization data from our previous study (Gnanagobal et al., 2021), we selected 28 and 98 dpi to represent early and chronic infection stages of *R. salmoninarum* in lumpfish, respectively, for sampling and transcriptome analyses. For instance, since lumpfish at 28 dpi had significantly higher *R. salmoninarum* loads in the head kidney and demonstrated mortality, we chose 28 dpi to reflect early infection. On the other hand, we reasoned 98 dpi to be ideal for representing chronic infection as lumpfish at this point had a considerable amount of chronically persisted *R. salmoninarum* loads without any mortality or clinical signs of BKD.

Fish from infected and control tanks ($n = 5$ per tank) were sampled at 1, 14, 28, 42, 56, and 98 dpi. Fish were euthanized with MS222 (400 mg L^{-1}; Syndel Laboratories, Vancouver, BC, Canada). Blood samples (1 mL) were taken from all five fish by puncturing the caudal vein and centrifuged at 10,000 rpm for 5 min at 4 °C to collect serum. The serum samples were stored at −80 °C until lysozyme activity assay and ELISA were performed. In order to provide an understanding of the lumpfish head kidney transcriptome response to *R. salmoninarum* at early and chronic infection stages, head kidney samples (~50–100 mg of tissue) were aseptically collected from control ($n = 3$) and infected ($n = 3$) fish at 28 and 98 dpi, placed in a 1.5 mL RNase-free tube, flash-frozen using liquid nitrogen, and kept at −80 °C until RNA extraction.

2.4. Lumpfish head kidney transcriptome profiling by RNA-sequencing

2.4.1. RNA extraction

Total RNA from head kidney samples was extracted using TRIzol reagent (Invitrogen) and purified with the RNeasy MinElute Cleanup Kit (QIAGEN, Mississauga, ON, Canada) following the manufacturer's instructions. Head kidney tissues (80–100 mg) were TRIzol-lysed using RNase-free motorized Pellet Pestle Grinder (Fisherbrand, Fisher Scientific, USA) prior to total RNA extraction. To remove residual genomic DNA, RNA samples were treated with TURBO DNA-free™ Kit (Invitrogen) following the manufacturer's recommendations. Purified RNA samples were quantified using a Genova Nano microvolume spectrophotometer (Jenway, UK) and assessed for integrity by 1% agarose gel electrophoresis. RNA samples used in transcriptome and qPCR analyses of this study showed acceptable integrity (i.e., tight 28S and 18S ribosomal RNA bands at a 2:1 ratio) and purity (i.e., A260/230 > 2.0 and A260/280 > 1.8).

2.4.2. Library preparation and RNA-seq

RNA from head kidney samples of 3 fish in the control group and 3 fish in the *R. salmoninarum* infected group at 28 and 98 dpi were subjected to RNA-seq analyses (i.e., 12 samples in total) (Fig. 1A and Supplementary Fig. 1A). RNA quality was determined using a NanoDrop spectrophotometer (Thermo Scientific) and Bioanalyzer 2100 (Agilent), and samples with an RNA integrity number (RIN) of 8 or above were used to build the libraries (Supplementary Table S1). Genome Quebec, QC, Canada constructed cDNA libraries using the NEBNext® Multiplex Oligos for Illumina® and performed paired-end sequencing on an Illumina NovaSeq 6000 platform with 100 bp read length. The current study's RNA-seq raw data are deposited in NCBI Sequence Read Archive (SRA) database under the bioproject accession number PRJNA978536.

2.4.3. RNA-seq data analyses

RNA-seq data were examined in CLC Genomics Workbench v20.0 (CLCGWB; Qiagen, Hilden, Germany) using settings similar to those previously reported (Chakraborty et al., 2022). Following the removal of poor-quality reads, clean paired reads were produced. Then, reads comprising adapters were trimmed employing the trim reads tool in CLCGWB. FastQC (https://www.bioinformatics.babraham.ac.uk/projects/fastqc/) and multiQC (Ewels et al., 2016) were used for the quality assessment of reads prior to and following trimming, respectively. CLCGWB mapped the trimmed high-quality reads against the lumpfish reference genome (Accession: PRJNA625538) using the RNA-seq analysis program. Gene expression was measured and mapped read counts were normalized using the RESM and eXpress methods (Li et al., 2010; Teng et al., 2016). After normalization, the counts allocated to each transcript were then used to generate the transcript per million reads (TPM) values using the trimmed mean of M-values (TMM) (Pereira et al., 2018). Global correlation analysis (e.g., Pearson method) and hierarchical clustering were performed on each gene's log_2-transformed TPM values (x+1) under control and *R. salmoninarum*-infected conditions at 28 and 98 dpi. The differential expression tool in CLCGWB, which is

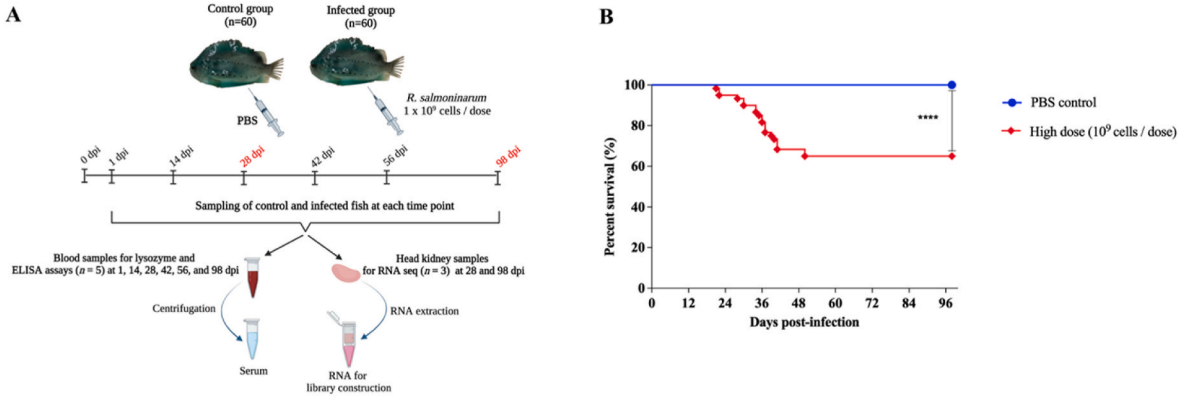

Fig. 1. Experimental infection and cumulative mortality. **(A)** Experimental design for *R. salmoninarum* infection in lumpfish and sampling. **(B)** Cumulative mortality in control and high-dose *R. salmoninarum* infected groups.

based on a negative binomial general linear model (GLM), was used to analyze differential gene expression of abundance data (Robinson et al., 2010). Biologically significant differentially expressed genes (DEGs) were identified using the standard cut-off values of $\log_2$ fold-change (FC) $\geq |1|$ and false discovery rate (FDR) $p \leq 0.01$ (Supplementary File S1A-D).

2.4.4. GO (Gene ontology) enrichment analyses and visualization of GO term networks

To understand the biologically relevant lumpfish immune responses modulated by the Gram-positive pathogen *R. salmoninarum* at early (28 dpi) and chronic (98 dpi) infection stages, selected DEGs from the reference-based transcriptomic assembly were subjected to GO term enrichment analyses using ClueGO (v2.5.9) and CluePedia plugins in Cytoscape (v3.9.0) (Bindea et al., 2009; Shannon et al., 2003). The ClueGO source file for lumpfish was used (Chakraborty et al., 2022).

First, to obtain an overall host-centric point of view based on enriched GO terms at each infection stage (i.e., early and chronic), the enrichment (i.e., right-sided hypergeometric test) analysis was performed on lists of DEGs (i.e., 1971 DEGs at 28 dpi and 139 DEGs at 98 dpi) (Supplementary File S1C, D) using the Benjamini-Hochberg method for *p*-value corrections ($p < 0.001$ for 28 dpi and $p < 0.01$ for 98 dpi), kappa-statistics score threshold of 0.5, and medium network specificity in ClueGO.

ClueGO generates networks of terms with related functions by using kappa-statistics to link the enriched Biological Processes (BP) GO terms (Cohen, 1968). The kappa-statistics scores (i.e., kappa-coefficient), which are computed for each term-term association based on the common genes between them, were used to define functional groupings of strongly-linked terms within the GO networks (Cohen, 1968; Eslamloo et al., 2020a). Since the kappa-statistic score cutoff is set at 0.5, term-term relationships with coefficient values below 0.5 would be considered non-significant. In addition, a GO term fusion approach was used to combine GO categories, reduce complexity, and build a functionally structured GO cluster network. The GO term with the lowest *p*-value was selected as the main term in each functional group for each cluster (represented by different colors). By considering the higher number of DEGs ($n = 1971$) at the early infection stage, a lower *p*-value (0.001) and the GO term fusion option were used in the enrichment analyses at 28 dpi in order to minimize the complexity of networks and to obtain a clear visualization of enriched terms.

Next, as previously described (Eslamloo et al., 2020a; Xue et al., 2021), the enriched GO terms were classified into five functional themes (i.e., cellular process, localization, and structure; metabolic process; development; immune response; response to stress) using the Gene Ontology Browser (http://www.informatics.jax.org) to further analyze the resulting networks at 28 dpi. The GO terms were grouped according to the biological process to which they were related and/or their parent terms.

Third, to explore the immune genes or pathways involved in the lumpfish host immune response against *R. salmoninarum* pathogenesis at the early infection stage (i.e., 28 dpi), the enrichment analysis was carried out on DEG lists (i.e., upregulated ($n = 434$) and downregulated genes ($n = 1537$) at 28 dpi) (Supplementary File S1E, F) using a right-sided hypergeometric test with the Benjamini-Hochberg method for *p*-value corrections ($p < 0.001$), kappa-statistics score cutoff of 0.5, GO term fusion option, and medium network specificity in ClueGO.

2.4.5. Correlation between RNA-seq and qPCR data

We previously reported the expression of 30 immune-relevant genes, including pattern recognition receptors, cytokines, innate and inflammatory immune response regulators, and humoral and cell-mediated immunity-related genes using qPCR analyses (Gnanagobal et al., 2021). Since we used the same RNA samples (i.e., 3 fish per time point from the control and infected groups, Total $n = 12$ samples) from our earlier qPCR study for the present RNA-seq, we compared the expression values from the RNA-seq data to the relative quantity (RQ) values obtained from qPCR to validate the results of the RNA-seq analysis. The QuantStudio Real-Time PCR Software-based (version 1.3) (Applied Biosystems) relative quantification study application was used to determine the RQ value of each sample for each gene after normalizing the C_T values to the levels of 2 reference genes (i.e., *pabpc1b* and *eif3d*). A correlation analysis was performed between the normalized counts (TPM+1) of RNA-seq data and the RQ values from qPCR analyses for the same 12 samples for the selected 30 genes. TPMs of RNA-seq data (Log_2 TPM+1 on the X axis) were plotted against RQs from qPCR ($\log_2$ RQ on the Y axis) on a scatter graph. Pearson correlation coefficients (R^2; $p < 0.05$) from simple linear regression analysis were used to compare the correlation between RNA-seq and qPCR analyses.

2.5. Fluorescence-based lysozyme activity assay

Lysozyme levels in lumpfish serum at 1, 14, 28, 42, 56, and 98 dpi were determined using a fluorescence-based lysozyme activity assay kit (Abcam, Waltham, MA, USA) following the manufacturer's instructions. This ultrasensitive assay measures the lysozyme activity by using the ability of lysozyme (Muramidase or N-acetylmuramide glycanhydrolase) (Ng et al., 2013) to cleave a synthetic substrate (4-Methylumbelliferone: 4-MU) and release a free fluorophore which can be quantified at Excitation/Emission (Ex/Em) of 360/445 nm at 37 °C in a fluorescent microplate reader. The increase in the fluorescence yield is proportional to the amount of active lysozyme in the serum samples.

Standard curve dilutions ranging from 20 to 100 pmol/well in a final volume of 50 μL were prepared in triplicate using a 10 μM 4-MU standard. Serum samples were centrifuged at 12,000×*g* for 5 min at 4 °C to discard any debris and diluted 1:10,000 in lysosome assay buffer to fit standard curve readings (i.e., sample readings should not be greater than that of the highest standard and must fall within the standard curve value range). Standards (50 μL), samples (40 μL), sample background controls (40 μL), reagent background control (40 μL), and positive control (40 μL) were randomly added to 96 well opaque white microplates (Falcon™, Fisher Scientific, Ottawa, ON, Canada). For substrate hydrolysis, 10 μL of the lysozyme substrate mix was added to each sample and positive control wells only and thoroughly mixed. Then, the plate was incubated at 37 °C for 60 min in the dark. After incubation, 50 μL of lysozyme stop buffer was added to all wells. The fluorescence was measured immediately on a fluorescent microplate reader (SpectraMax M5 Multi-Mode Microplate Reader, Molecular Devices, Sunnyvale, CA, USA) at Ex/Em of 360/445 nm at 37 °C in endpoint mode with 5 s of plate shaking before reading.

Corrected fluorescence values were obtained by subtracting the mean fluorescence value of the blank (standard of 0 pmol/well) from standard and sample readings. In addition, sample background readings were also deducted from the sample readings. A standard curve was generated by plotting the readings of the standards ranging from 0 to 100 pmol/well and drawing the line of the best fit. The trend line equation that provided the most accurate fit was calculated in order to get the amount of 4-MU generated during the reaction. For example, the variation in the fluorescence of each sample after deducting blank and sample background control values was applied to the standard curve trend line equation to determine the amount of 4-MU in the sample well. Lysozyme activity (pmol/minute/mL) in each sample was calculated as follows:

$$\textit{Lysozyme activity} = \left(\frac{B}{\Delta T \times V}\right) \times D$$

B = Amount of 4-MU in the sample well calculated from the standard curve (pmol); ΔT = Reaction time (min); V = Sample volume per well; D = Sample dilution factor.

2.6. Indirect enzyme-linked Immunosorbent assay (ELISA)

Indirect ELISA was used to measure the *R. salmoninarum*-specific lumpfish antibody titers at 14, 28, 42, 56, and 98 dpi. Initially, serum samples (5 control and 5 infected fish per time point) were incubated at 56 °C for 30 min in a water bath to inactivate the complement components. Subsequently, 100 μL of chloroform were added to the heat-treated serum samples and kept for 10 min at room temperature to dissolve fats. Finally, samples were centrifuged at 4000×*g* for 5 min at room temperature, supernatants were extracted and transferred into clean microfuge tubes. A new checkerboard titration by indirect ELISA method (as described below) was performed to identify the optimal antigen concentration (Formalin-killed *R. salmoninarum* cell antigen) to react with lumpfish serum (Crowther, 2000). The *anti-R. salmoninarum* antibodies in the lumpfish serum were determined using 6 different antigen concentrations (4, 2, 1, 0.5, 0.25, 0.125 μg/mL) to react with 6 two-fold serial dilutions of a pool of serum from control and *R. salmoninarum* infected lumpfish (1:2 to 1:64). First, microplate (Corning Costar, Waltham, MA, USA) wells were coated with different antigen concentrations and incubated overnight at 4 °C. The wells were washed 3 times with PBS-Tween and blocked with 150 μL of ChonBlock™ for 1 h at 37 °C, washed 3 times, and incubated with different dilutions of control and *R. salmoninarum* infected lumpfish serum in PBS-Tween for 1 h at 37 °C. From the checkerboard titration, 4 μg/mL was selected as an optimal antigen concentration for the experimental indirect ELISA.

For the experimental indirect ELISA, each well of the 96 well microtiter plates was coated with 100 μL (4 μg/well) of formalin-killed *R. salmoninarum* cell antigen diluted in coating buffer (0.015 mM Na_2CO_3; 0.035 mM $NaHCO_3$; pH 9.8) and incubated at 4 °C overnight. Unbound antigen in the coated plates was removed by washing the wells 3 times with PBS containing 0.1% Tween-20 (PBS-Tween). To block antigen uncoated sites, 150 μL of ChonBlock™ blocking buffer (Chondrex Inc, Woodinville, WA, USA) was added to each well and incubated for 1 h at 37 °C. After washing the plate 3 times with PBS-Tween, the wells were incubated with 8 two-fold serial dilutions of control ($n = 5$) and *R. salmoninarum* infected ($n = 5$) lumpfish serum (1:2 to 1:256 in PBS-Tween) for 1 h at 37 °C and washed 5 times with PBS-Tween. One hundred microliters of chicken IgY anti-lumpfish IgM (secondary antibody) (Gendron et al., 2020) diluted to 1:10,000 in PBS-Tween were subsequently added to all tested wells, incubated for 1 h at 37 °C, and washed 5 times with PBS-Tween. Later, 100 μL of streptavidin-HRP (Southern Biotech, Birmingham, AL, USA) diluted to 1:10,000 in PBS-Tween was added to each well and incubated for 1 h at 37 °C. After washing 3 times with PBS-Tween at room temperature, 50 μL of ultra TMB (1-Step™ Ultra TMB-ELISA substrate solution, Thermofisher Scientific, Rockford, IL, USA) was added to the wells, incubated at room temperature for 30 min, and the colorimetric reaction was stopped by adding 50 μL of 2M H_2SO_4. The O.D. was read at 450 nm on a microplate reader (SpectraMax M5 Multi-Mode Microplate Reader, Molecular Devices, Sunnyvale, CA, USA). To choose the optimal serum dilution cut-off, the highest dilution of the serum, after which the O. D values started to increase with the increasing dilution factor, was taken as the specific antibody titer and normalized to logarithmic base two scale.

2.7. Statistical analysis

Statistical analysis and data visualization were carried out in Prism package v7.0 (GraphPad Software, La Jolla, CA, USA), and a *p*-value ≤ 0.05 was regarded as statistically significant. Survival rates of control and *R. salmoninarum* infected groups were calculated using the Kaplan-Meier estimator and compared using the Log-rank test. Lysozyme activity and indirect ELISA results were analyzed using a two-way ANOVA test and Sidak multiple comparisons test to determine significant differences between treatments (i.e., control and infected groups) and time points (i.e., 1, 14, 28, 42, 56, 98 dpi). Simple regression analysis was conducted to determine the correlation between TPM and RQ values.

3. Results

3.1. Global transcriptome profile of lumpfish head kidney at early and chronic R. salmoninarum infection stages

To study the lumpfish head kidney response to *R. salmoninarum* at early and chronic infection stages, the global transcriptomic profiles of lumpfish head kidney at 28 and 98 dpi were explored using RNA-seq and reference-based transcriptome assembly analysis (Supplementary Fig. S1A). Information on RNA-seq data quality and sequencing statistics is provided in Supplementary Tables 1 and 2, and Supplementary Fig. S1B.

Global correlation analyses showed a high degree of expression correlation under different experimental conditions, for instance, R^2 of 0.95 and 0.97 ($p < 0.0001$) were observed between control and *R. salmoninarum* infected fish groups at 28 and 98 dpi, respectively (Supplementary Figs. S1C and D). Principal component analysis (PCA) and hierarchical clustering analyses (i.e., heat map) showed clear differences between control and infected samples at 28 dpi (Fig. 2A–C). Contrarily, despite the fact that the control and infected samples were segregated at 98 dpi, their clusters in the PCA had a minor overlap, which also matched the heat map (Fig. 2B–D). The transcriptome dysregulations in the lumpfish head kidney were stronger and more extensive at 28 dpi (Fig. 2E) compared to 98 dpi (Fig. 2F). In agreement with this, the number of statistically significant DEGs in the lumpfish head kidney at 28 dpi (1971) was higher compared to 98 dpi (139) (Fig. 2G). Among 1971 DEGs at 28 dpi, 434 genes were upregulated, and 1537 genes were downregulated. On the other hand, total DEGs at 98 dpi included 125 upregulated and 14 downregulated genes. As shown in the Venn diagram, there were 80 genes (10 up- and 70 down-regulated at 28 dpi, 75 up- and 5 down-regulated at 98 dpi) overlapping between gene lists at both time points 28 and 98 dpi (Fig. 2G). Gene identifier, description, fold change, and FDR *p*-value at 28 and 98 dpi were listed in Supplementary File S1A-N.

3.2. Pathway enrichment analyses

To study host molecular pathways regulated by *R. salmoninarum* infection, we used ClueGO and identified the enriched GO terms related to biological processes (BP), molecular functions (MF), and cellular components (CC) of significant *R. salmoninarum*-responsive DEGs lists in lumpfish head kidney at 28 and 98 dpi.

First, we tested the BPs, MFs, and CCs over-represented in the total up- and down-regulated lists of DEGs at 28 ($n = 1971$) and 98 ($n = 139$) dpi (Supplementary File S1C and S1D) to obtain an overall host-centric point of view. The enriched GO terms identified herein for 28 dpi were further classified into functional themes using Gene Ontology Browser. For instance, we identified 167 GO terms enriched ($p < 0.001$) in *R. salmoninarum*-responsive genes in the lumpfish head kidney at 28 dpi (Fig. 3A; Supplementary Table S3). These enriched GO terms were associated with cellular process, localization, and structure (63%), metabolic process (25%), immune response (7%), response to stress (3%), and development (2%) (Fig. 3A). When examining BPs, MFs, and CCs over-represented in the total up- and down-regulated lists of DEGs ($n = 139$) in the lumpfish head kidney at 98 dpi (Supplementary File S1D), we found only 21 GO terms enriched ($p < 0.01$) in *R. salmoninarum*-responsive genes (Fig. 3B; Supplemental Table S4). Chronic infection with *R. salmoninarum* in lumpfish at 98 dpi triggered dysregulation of several BPs relevant to adaptive immunity. This involved immune response to tumor cells and its regulation (e.g., T cell-mediated cytotoxicity directed against tumor cell target), and antigen presentation process (e.g., antigen processing and presentation of peptide antigen via MHC class I). In addition, other BPs enriched in the lumpfish head kidney at 98 dpi were involved in antioxidant activity (e.

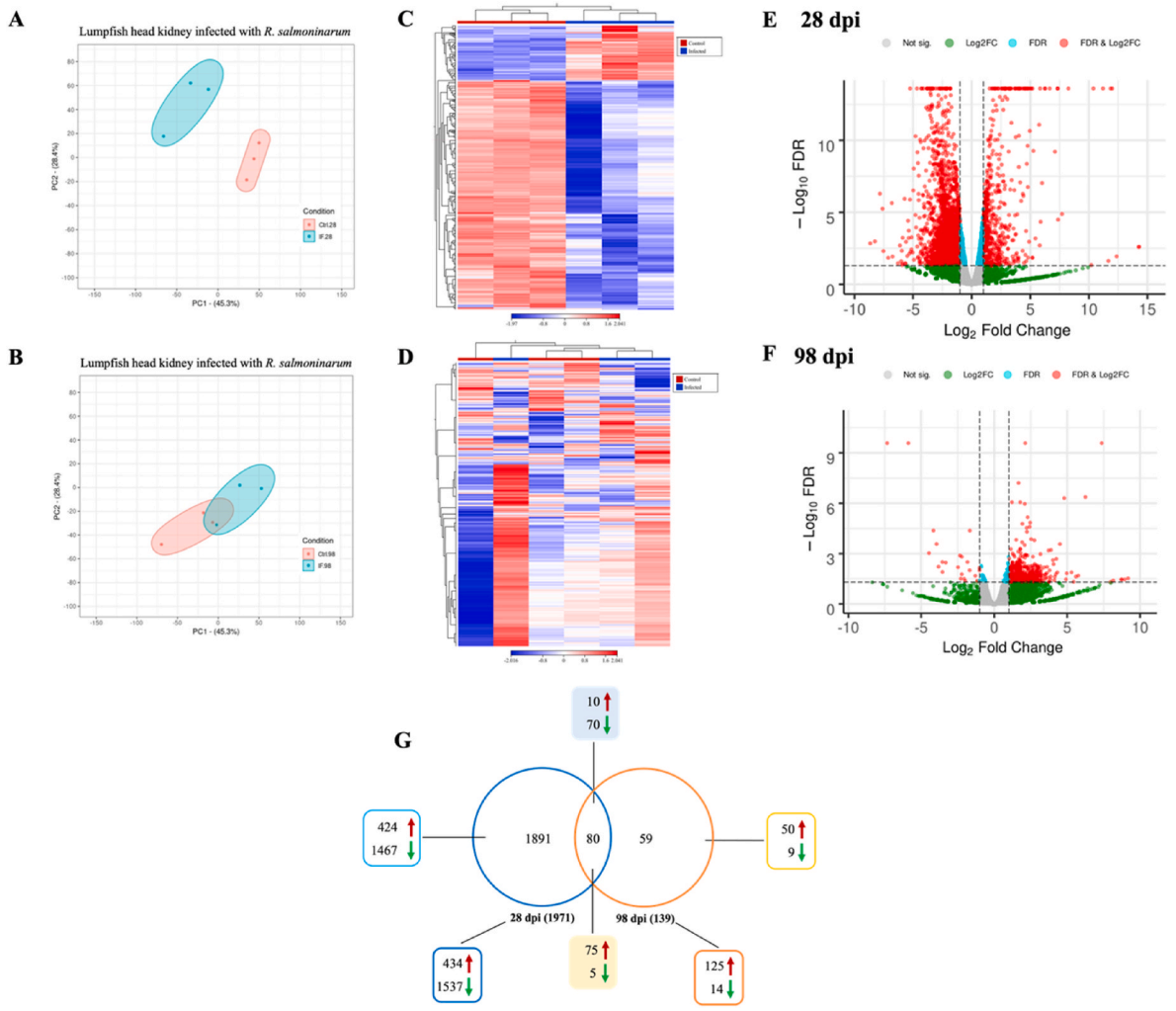

Fig. 2. Global transcriptomic profiling of the lumpfish head kidney response to *R. salmoninarum* at early (28 dpi) and chronic (98 dpi) infection stages by RNA-seq. A total of 12 RNA libraries comprised of 3 biological replicates for 2 different conditions (control and *R. salmoninarum* infected head kidney samples at 28 and 98 dpi) were included in the RNA-seq analyses. Principal component analysis (PCA) of control (Ctrl) and *R. salmoninarum* infected (IF) head kidney samples at (**A**) 28 dpi and (**B**) 98 dpi. Hierarchical clustering of differentially expressed genes (DEGs); color bars below the horizontal cluster indicate control (red) and *R. salmoninarum* infected head kidney samples (blue) at (**C**) 28 dpi and (**D**) 98 dpi. Volcano plots of DEGs at (**E**) 28 dpi and (**F**) 98 dpi. Red dots indicate significant DEGs. (**G**) Venn Diagram (Genes) showing an overview of RNA-seq results between early (28 dpi) and chronic infection (98 dpi) stages. Blue and orange circles represent 28 and 98 dpi, respectively, whereas red and green arrows indicate up- and down-regulated genes, respectively. (For interpretation of the references to color in this figure legend, the reader is referred to the Web version of this article.)

g., glutathione peroxidase activity), osmoregulation (e.g., regulation of water loss via skin), and organic substance metabolic process (e.g., glutathione metabolic process).

Second, we examined the BPs, MFs, and CCs over-represented in individual up- ($n = 434$; Supplementary File S1E) and down-regulated ($n = 1537$; Supplementary File S1F) DEG lists at 28 dpi to investigate specific immune pathways or genes involved in the lumpfish immune response against *R. salmoninarum* pathogenesis. Here, 93 and 160 GO terms were enriched ($p < 0.001$) in the individual up- (Fig. 4A; Supplementary Table S5) and down-regulated (Fig. 4B; Supplementary Table S6) genes list, respectively, at 28 dpi.

Among the upregulated genes at 28 dpi, GO terms associated with several innate and adaptive immune processes were enriched (Fig. 4A; Supplementary Table S5). A large number of BPs associated with the innate immune response (e.g., acute phase response, cytokine/chemokine activity, complement activation, defense response to bacterium) and regulation of immune response (e.g., negative regulation of IL-8 production, cellular iron ion homeostasis, regulation of nitric-oxide biosynthesis/phagocytosis) were activated (Supplementary Table S5). The BPs enriched that were linked to the adaptive immune response include lymphocyte activation/differentiation/migration (e.g., natural killer cell activation/differentiation, negative regulation of T cell differentiation, $CD4^+$ α-β T cell activation/differentiation/positive regulation, lymphocyte chemotaxis, negative regulation of lymphocyte activation and leukocyte differentiation, mononuclear cell migration), adaptive immunity-related cytokine responses (e.g., negative regulation of interferon-gamma (IFN-γ) and IL-6 production), B-cell, (e.g., antimicrobial humoral immune response, immunoglobulin (Ig) production/regulation, positive regulation of B-cell proliferation, Ig-mediated immune response) and T-cell mediated (e.g., T-helper 1 type and T-helper 17 type immune responses, positive regulation of T cell proliferation) adaptive immune responses. Furthermore, we identified induction of immune pathways linked to complement activation (e.g., alternative pathway), cell death (e.g., positive regulation of leukocyte apoptotic process), and Janus kinase (JAK)-Signal transducer and activator of transcription (STAT) signalling (e.g., positive regulation of receptor signaling pathway via STAT, 1-phosphatidylinositol-3-kinase regulator activity) in response to *R. salmoninarum* infection at 28 dpi (Supplementary Table S5).

On the other hand, most of the BPs that were found to be enriched in

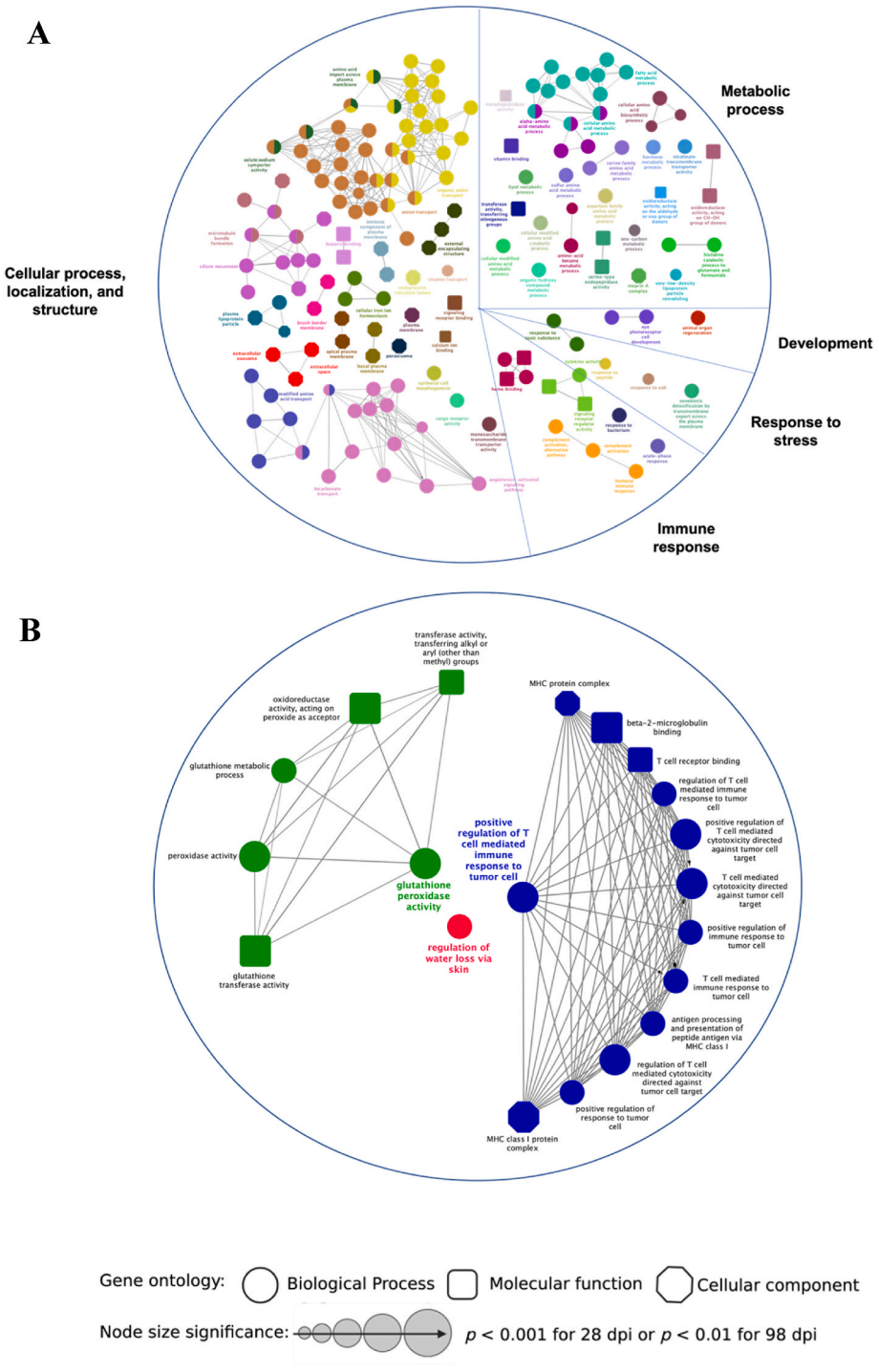

Fig. 3. Global view of ClueGO-based gene ontology enrichment networks in lumpfish head kidney at (**A**) 28 and (**B**) 98 dpi. The enrichment (i.e., right-sided hypergeometric test) analysis was performed on lists of DEGs (i.e., 1971 DEGs at 28 dpi and 139 DEGs at 98 dpi) that contain total up- and down-regulated genes using Benjamini-Hochberg method for *p*-value corrections ($p < 0.001$ for 28 dpi and $p < 0.01$ for 98 dpi), kappa-statistics score threshold of 0.5, and medium network specificity in ClueGO. A significantly enriched Gene Ontology (i.e., GO) is represented by each node. The functional groups and processes that share similar genes are visualized using the node color regime. Each functional group's most significantly enriched terms are denoted by a summary label (i.e., the leading GO term based on the highest significance is represented using a name label). The GO term shapes, ellipse, rounded rectangle, and octagon represent BPs, MFs, and CCs, respectively. The shape size corresponds to the significance of the GO term or enriched pathway. For instance, the larger the size of the shapes, the higher the significance. The complete lists of GO terms and statistics (over-represented BPs, MFs, and CCs) are tabulated in Supplementary Tables S3 and S4. (For interpretation of the references to color in this figure legend, the reader is referred to the Web version of this article.)

the downregulated genes list at 28 dpi (Fig. 4B; Supplementary Table S6) were associated with metabolism and cellular processes, particularly related to the amino acid metabolism (e.g., histidine catabolic process to glutamate and formamide/formate, the metabolic process of amino acids (betaine, carnitine, glutamate, glycine, dicarboxylic acid, serine family, glutamine family, aspartate family, cellular amino acid, cellular modified amino acid), the catabolic process of cellular, sulfur, and alpha-amino acids, and the biosynthetic process of

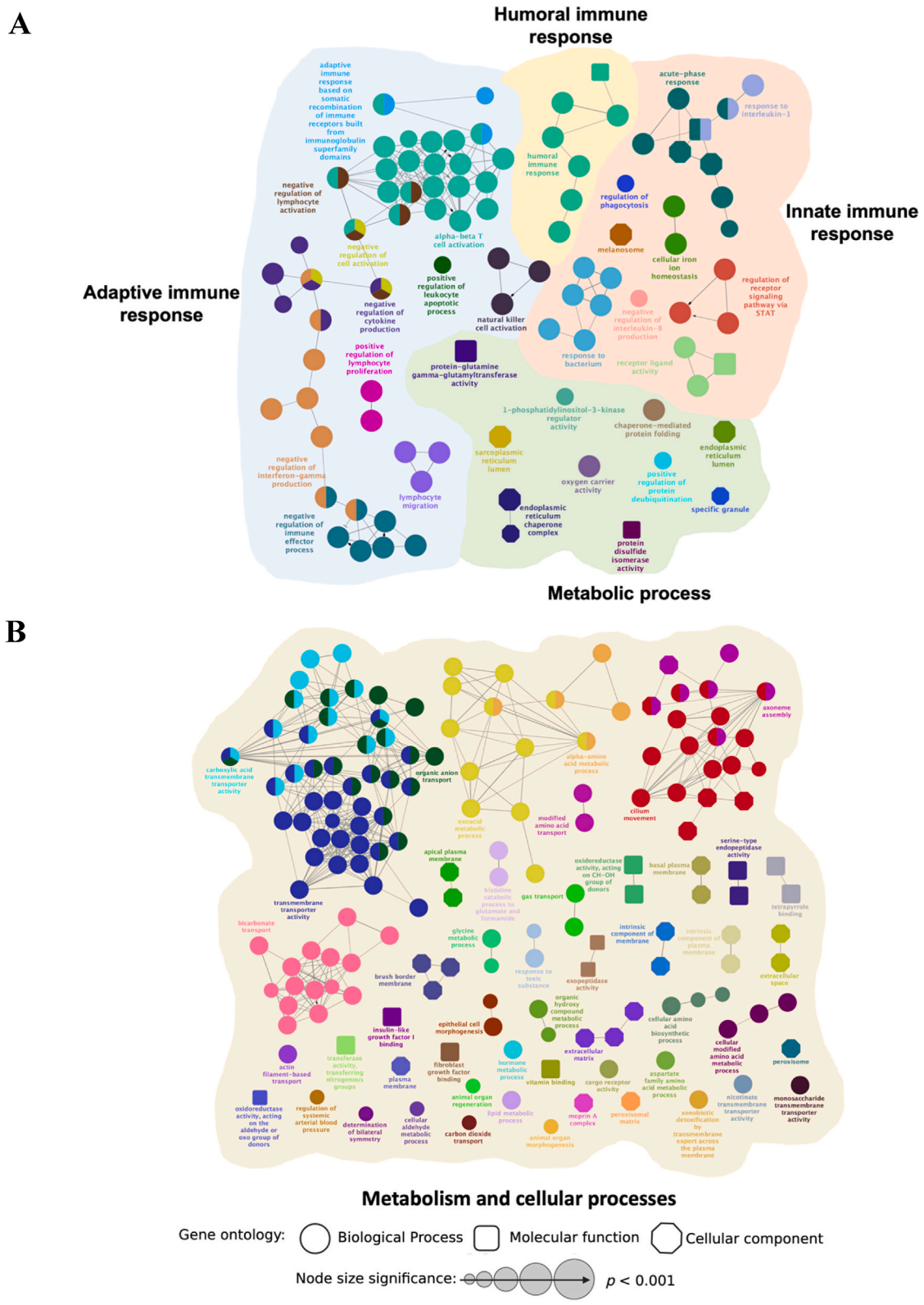

Fig. 4. ClueGO-based enriched gene ontology terms of all (**A**) upregulated and (**B**) downregulated genes in lumpfish head kidney at 28 dpi. The enrichment analysis was carried out on DEG lists (i.e., upregulated ($n = 434$) and downregulated genes ($n = 1537$) at 28 dpi) using a right-sided hypergeometric test with the Benjamini-Hochberg method for *p*-value corrections ($p < 0.001$), kappa-statistics score cutoff of 0.5, GO term fusion option, and medium network specificity in ClueGO. A significantly enriched Gene Ontology (i.e., GO) is represented by each node. The functional groups and processes that share similar genes are visualized using the node color regime. Each functional group's most significantly enriched terms are denoted by a summary label (i.e., the leading GO term based on the highest significance is represented using a name label). The GO term shapes, ellipse, rounded rectangle, and octagon represent BPs, MFs, and CCs, respectively. The significance of the GO term or enriched pathway is expressed by the size of the GO term shapes (i.e., the larger the size of the shapes, the higher the significance). The complete lists of GO terms and statistics (over-represented BPs, MFs, and CCs) are tabulated in Supplementary Tables S5 and S6. (For interpretation of the references to color in this figure legend, the reader is referred to the Web version of this article.)

cellular and alpha-amino acids).

Overall, in the lumpfish head kidney at the early infection stage (28 dpi), *R. salmoninarum*-induced (i.e., upregulated) genes were mainly involved in innate and adaptive immune response-related pathways, whereas *R. salmoninarum*-suppressed (i.e., downregulated) genes were largely connected to amino acid metabolism, cellular and developmental processes. On the other hand, *R. salmoninarum* dysregulated the genes involved in T-cell mediated cytotoxicity and MHC-I pathway in lumpfish head kidney at the chronic infection stage (98 dpi).

Table 1
Selected DEGs associated with enriched pathways of interest from ClueGO analyses at 28 and 98 dpi.

Enriched pathway of interest	Gene Symbol	Log_2 Fold change	FDR p-value	Putative protein product
28 dpi				
Response to bacterium	*tlr5*	2.40	4.2×10^{-6}	Toll-like receptor 5
	pglyrp6	6.65	0	Peptidoglycan recognition protein 6
	si:ch73-86n18.1	1.45	6.3×10^{-7}	C-type lectin domain family 4 member E
	mapkapk3	1.24	1.3×10^{-5}	MAP kinase-activated protein kinase 3
	si:ch211-152p11.4	−2.06	5.0×10^{-4}	Regulator of G-protein signaling 3 isoform X1
	inavaa	−2.17	8.9×10^{-4}	Innate immunity activator protein
Cytokine/Chemokine activity	*LOC117736885*	6.24	0	Interleukin-1 beta-like
	cxcl8a	4.75	0	Interleukin-8 isoform X1
	tnfsf12	−2.47	1.7×10^{-12}	Tumor necrosis factor ligand superfamily member 12
	il10	4.03	4.8×10^{-11}	Interleukin-10
	LOC117727469	−1.90	9.9×10^{-6}	C–C motif chemokine 4-like
	cxcl19	1.72	5.6×10^{-5}	C-X-C motif chemokine 19
	LOC117736467	2.95	1.4×10^{-4}	C–C motif chemokine 13-like
	m17	1.84	2.6×10^{-4}	IL-6 subfamily cytokine M17
Acute phase response	*LOC117728776*	14.26	2.6×10^{-3}	Amyloid protein A-like
Cellular iron homeostasis	*LOC117728128*	11.99	0	Hepcidin-like
	hamp	7.32	0	Hepcidin-1
	hpxb	3.16	6.1×10^{-10}	Hemopexin
	tfr1b	1.30	1.2×10^{-6}	Transferrin receptor 1b
Complement activation, alternative pathway	*c7b*	4.52	0	Complement component C7
	LOC117729317	4.46	0	Complement factor H-like
	LOC117742524	4.02	7.2×10^{-9}	Complement factor B-like
	c6	3.37	0	Complement component C6
	LOC117745115	2.43	8.6×10^{-3}	Complement C3-like
Apoptosis	*card9*	1.08	6.0×10^{-6}	Caspase recruitment domain-containing protein 9
	LOC117734930	2.25	0	Cell death-inducing p53-target protein 1 homolog
	bcl3	1.61	3.7×10^{-8}	B-cell lymphoma 3 protein homolog isoform X1
Humoral and cell immunity	*LOC117732554*	1.04	3.0×10^{-3}	B-cell receptor CD22-like isoform X2
	LOC117750771/ctla4	2.44	2.4×10^{-3}	Cytotoxic T-lymphocyte protein 4-like
	LOC117727997/ siglec10	1.29	6.8×10^{-6}	Sialic acid-binding Ig-like lectin 10 isoform X1
	LOC117739425	5.09	0	Tumor necrosis factor receptor superfamily member 6B-like
	tnfaip3	1.08	5.8×10^{-5}	Tumor necrosis factor alpha-induced protein 3 isoform X1
	mertka	1.42	1.1×10^{-10}	Tyrosine-protein kinase Mer isoform X2
	ebi3	1.97	1.8×10^{-4}	Interleukin-27 subunit beta
	tap2a	1.27	9.0×10^{-6}	Antigen peptide transporter 2a
JAK-STAT signalling pathway	*LOC117739248/il6*	4.70	4.3×10^{-9}	Interleukin-6-like
	LOC117750018/il10rb	1.18	7.4×10^{-7}	Interleukin-10 receptor subunit beta-like
	socs3a	3.96	0	Suppressor of cytokine signaling 3a
	cish	3.92	0	Cytokine-inducible SH2-containing protein
Amino acid metabolism	*hal*	−2.55	1.2×10^{-8}	Histidine ammonia-lyase
	LOC117740696	−5.88	5.9×10^{-4}	Betaine–homocysteine S-methyltransferase 1-like
	adhfe1	−2.23	9.3×10^{-14}	Hydroxyacid-oxoacid transhydrogenase, mitochondrial
	gcshb	−3.38	3.2×10^{-13}	Glycine cleavage system protein H (aminomethyl carrier), b
	agxtb	−2.61	8.8×10^{-8}	Alanine–glyoxylate and serine–pyruvate aminotransferase b
	LOC117727751	−3.13	8.7×10^{-4}	Rho GTPase-activating protein 11A-like
	LOC117733571	−4.10	0	Serine hydroxymethyltransferase, mitochondrial-like isoform X1
	ddo	−2.91	6.2×10^{-10}	d-aspartate oxidase
	got1	−2.50	2.1×10^{-8}	Aspartate aminotransferase, cytoplasmic
	gls2b	−2.16	2.0×10^{-6}	Glutaminase 2b isoform X2
98 dpi				
T cell-mediated immunity/MHC-class I	*LOC117738775*	2.29	6.7×10^{-6}	Major histocompatibility complex class I-related gene protein-like isoform X2
	LOC117739375	2.52	1.4×10^{-4}	H-2 class I histocompatibility antigen, Q9 alpha chain-like
Glutathione peroxidase activity	*LOC117725889*	1.92	1.7×10^{-5}	Microsomal glutathione S-transferase 1-like
	gpx3	1.32	7.0×10^{-3}	Glutathione peroxidase 3 isoform X1
	gsta.1	1.24	3.5×10^{-3}	Glutathione S-transferase, alpha tandem duplicate 1
	gstt1a	1.50	1.5×10^{-4}	Glutathione S-transferase theta-1a

3.3. DEGs associated with the enriched GO terms of interest at 28 and 98 dpi

To generally understand the molecular pathways regulated by *R. salmoninarum* infection at the gene level, selected DEGs associated with enriched GO terms of interest from ClueGO analyses at 28 and 98 dpi are tabulated in Table 1.

In the enriched term "response to bacterium" at 28 dpi, *R. salmoninarum* infection upregulated pattern recognition receptors (PRR), including *toll-like receptor 5*, *peptidoglycan recognition protein 6*, and *C-type lectin domain family 4 member E*. Interestingly, a mitogen-activated protein kinase (MAPK) or extracellular signal-regulated kinase (ERK) that mediate intracellular signalling, *MAP-kinase-activated protein kinase 3* was upregulated, in contrast, a *regulator of G-protein signalling 3 isoform X1*, which is a GTPase-activating protein that inhibits G-protein-mediated signal transduction, was downregulated. Moreover, *R. salmoninarum* downregulated the expression of *innate immunity activator protein* (*inavaa*), which is crucial for PRR-induced signalling, cytokine release, and bacterial clearance.

Genes associated with cytokines or chemokines activity that were upregulated by *R. salmoninarum* infection in lumpfish head kidney at 28 dpi (Table 1; Supplementary Table S5) include *interleukin-1 beta-like*, *interleukin-8 isoform X1*, *interleukin-10*, *C-X-C motif chemokine 19*, *C–C motif chemokine 13-like*, and *IL-6 subfamily cytokine M17*. *R. salmoninarum* was also found to induce the expression of genes involved in acute phase response (*amyloid protein A-like*), iron homeostasis (*hamp1*), *hemopexin b*, *transferrin receptor 1b*), complement activation - alternative pathway (*complement component C7*, *complement factor H-like*, *complement component C6*, *complement C3-like*), regulators of apoptosis and NFkB (nuclear factor kappa light chain enhancer of activated B cells) activation (*cell death-inducing p53-target protein 1 homolog*, *caspase recruitment domain-containing protein 9*, *B-cell lymphoma 3 protein homolog isoform X1*), and JAK-STAT signalling pathway (*interleukin-6-like*, *interleukin-10 receptor subunit beta-like*, *suppressor of cytokine signaling 3a*, *cytokine-inducible SH2-containing protein*) in lumpfish at 28 dpi (Table 1).

Among the enriched GO terms associated with humoral and cell-mediated adaptive immunity at 28 dpi (Table 1; Supplementary Table S5), the genes play putative roles in the negative regulation of production of molecular mediators of immune response (*B-cell receptor CD22-like isoform X2*), negative regulation of T cell activation/differentiation *cytotoxic T-lymphocyte protein 4-like*), regulation of immunoglobulin production (*sialic acid-binding Ig-like lectin 10 isoform X1*), regulation of phagocytosis (*tyrosine-protein kinase Mer isoform X2*), T-helper 1 type immune response (*interleukin-27 subunit beta*), and MHC-1 mediated antigen processing and presentation (*antigen peptide transporter 2a*) showed upregulation in response to *R. salmoninarum*. Further, *R. salmoninarum* caused the downregulation of many genes involved in amino acid metabolism (biosynthesis/degradation) (Table 1; Supplementary Table S6).

Compared to 28 dpi, where a larger number of genes and pathways were dysregulated, only a lesser number of genes and pathways were dysregulated at 98 dpi (Table 1; Supplementary Table S4). For instance, *R. salmoninarum* chronic infection upregulated genes involved in T-cell mediated cytotoxicity and MHC-1 pathway (*major histocompatibility complex class I-related gene protein-like isoform X2*, *H-2 class I histocompatibility antigen*, *Q9 alpha chain-like*) in lumpfish head kidney at 98 dpi.

3.4. qPCR validation analysis

To validate the current RNA-seq results, correlation analyses were performed between the $\log_2$ of the TPM values from the RNA-seq and the $\log_2$ of the RQ values from our previous qPCR (Gnanagobal et al., 2021) for 30 genes. R^2 values of 0.8 or above are regarded as highly correlated (Everaert et al., 2017). R^2 values between 0.5 and 0.8 are regarded as having a medium level of correlation, while those below 0.5 are considered to have a low correlation. Among the 30 selected genes, 18 genes showed significantly high gene expression correlations (i.e., R^2 values ranged from 0.7987 to 0.9568; $p < 0.0001$), suggesting an overall high concordance between RNA-seq and qPCR data (Fig. 5 and Supplementary Table S7). Significant medium gene expression correlations were observed for 7 genes (i.e., R^2 values ranged from 0.4904 to 0.7128; $p < 0.001$, $p < 0.01$, and $p < 0.05$) (Supplementary Fig. S2 and Supplementary Table S7). Correlations between RNA-seq and qPCR data were poor and not significant for 5 genes (i.e., R^2 values ranged from 0.0922 to 0.2634) (Supplemental Fig. S2 and Supplementary Table S7). Overall, 83% of the qPCR-studied genes showed significant correlations (i.e., 25 out of 30 genes showed significantly high to medium levels of correlation with R^2 values ranging from 0.5 to 0.96; R^2 values of 0.5 and above were considered as significant correlation) with the current RNA-seq results.

3.5. Lysozyme activity in lumpfish serum

To determine changes in the lumpfish serum lysozyme levels during *R. salmoninarum* infection, a fluorescence-based lysozyme activity assay was used. The standard curve of the fluorescence-based activity assay is shown in Fig. 6A. The linear regression equation and the correlation coefficient for the standard curve were $Y = 43.65X + 55.83$ and $R^2 = 0.9985$, respectively (Fig. 6A). Fig. 6B displays the measurements of active lysozyme in lumpfish serum at 1, 14, 28, 42, 56, and 98 dpi. The serum lysozyme levels of the infected fish at earlier sampling (i.e., 1 dpi) were significantly higher ($p < 0.05$) compared to the control fish at 1 dpi. Compared to the infected fish at 1 dpi, lysozyme activity in serum had significantly declined in the infected fish at 98 dpi. However, on days 14, 28, 42, 56, and 98, lysozyme levels did not differ significantly between control and infected fish or between infected fish.

3.6. Specific serum antibody response

To examine the changes in the humoral antibody response in lumpfish serum during *R. salmoninarum* infection, specific serum antibody titers at 14, 28, 42, 56, and 98 dpi were measured using indirect ELISA. The $\log_2$ antibody titers were not significantly different between control and *R. salmoninarum* infected fish in all the tested time points (Fig. 6C).

4. Discussion

Lumpfish is a novel and economically important species for the salmon farming industry due to its use as cleaner fish to control sea lice (Powell et al., 2018). However, high mortality caused by bacterial infections is a challenge for lumpfish aquaculture (Brooker et al., 2018). Expanding our knowledge of the lumpfish immune system and its host-pathogen interactions is crucial to provide a basis for the development of efficient immune prophylactic measures. The current study is the first to describe the transcriptome response of lumpfish head kidney to *R. salmoninarum* at early (28 dpi) and chronic (98 dpi) infection stages.

Our RNA-seq results found extensive *R. salmoninarum*-dependent dysregulation of several genes involved in immune responses, metabolism, cellular process, development, and response to stress in lumpfish head kidney at 28 dpi compared to 98 dpi (Fig. 2E and F and Fig. 3A). To be specific, upregulated genes in response to *R. salmoninarum* infection at 28 dpi were mainly involved in innate and adaptive immunity, whereas downregulated genes were mostly associated with amino acid metabolism (i.e., biosynthesis and degradation of amino acids), cellular and developmental processes (Fig. 4). However, the lumpfish transcriptional response to this pathogen at 98 dpi was remarkably low, where *R. salmoninarum*-dependent dysregulation of genes was largely linked to cell-mediated adaptive immunity (Fig. 3B). The samples from the control ($n = 3$) and *R. salmoninarum*-infected ($n = 3$) fish at 28 and

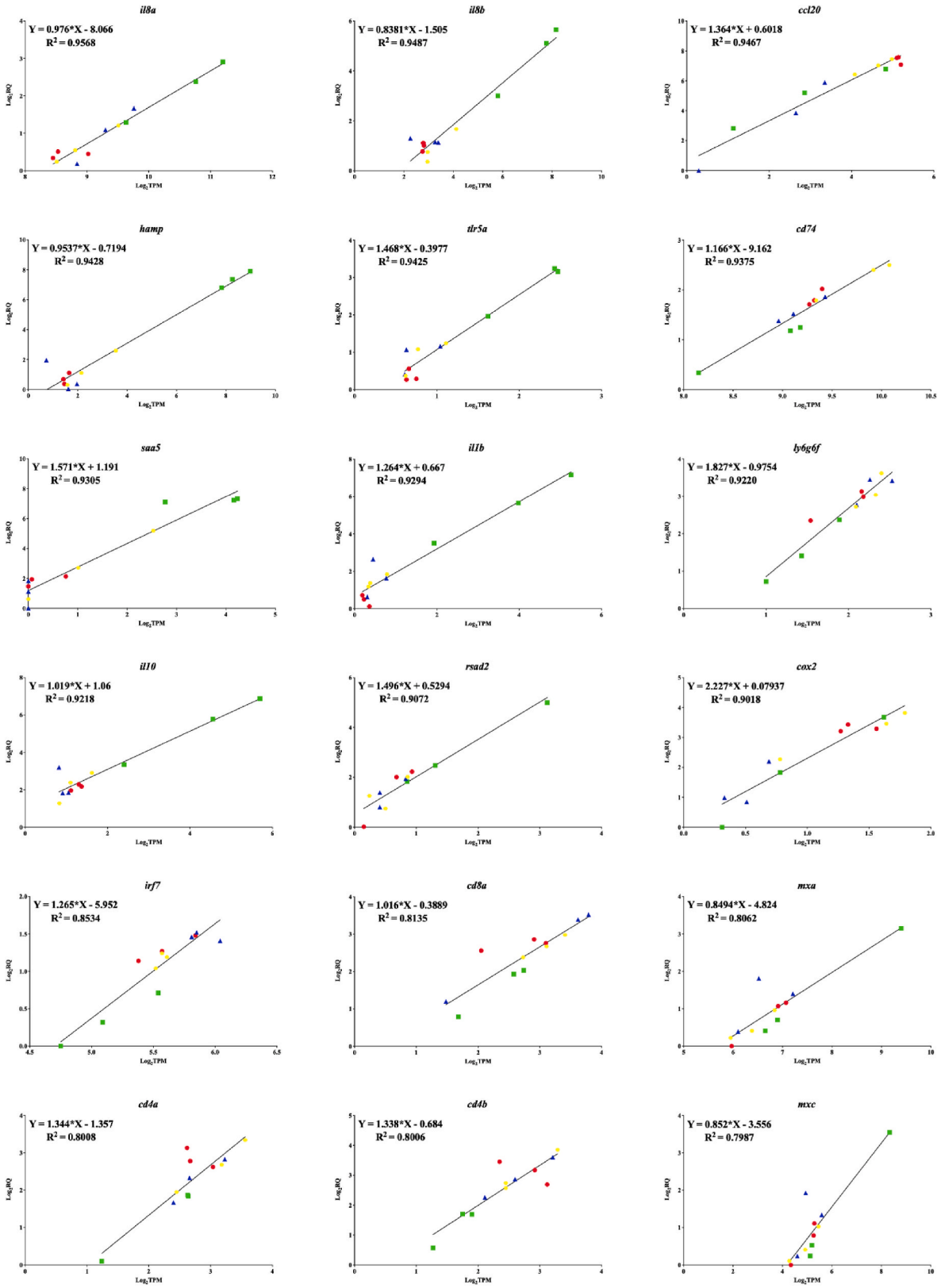

Fig. 5. Gene expression correlation (high) between qPCR and RNA-seq data for 18 genes of interest. RNA-seq data are presented as $\log_2$TPM (X axis). These 18 genes showed a significantly high correlation (level of significance: $p < 0.0001^{****}$) with the current RNA-seq results. qPCR data are represented as $\log_2$RQ (Y axis). The red circles represent control samples at 28 dpi; the green squares represent *R. salmoninarum*-infected samples at 28 dpi; the blue triangles represent control samples at 98 dpi; the yellow hexagons represent *R. salmoninarum*-infected samples at 98 dpi. Each symbol is an average of the three fish at a particular time point in the head kidney tissue. The linear regression equation and the correlation coefficient (R^2) are indicated for each gene. (For interpretation of the references to color in this figure legend, the reader is referred to the Web version of this article.)

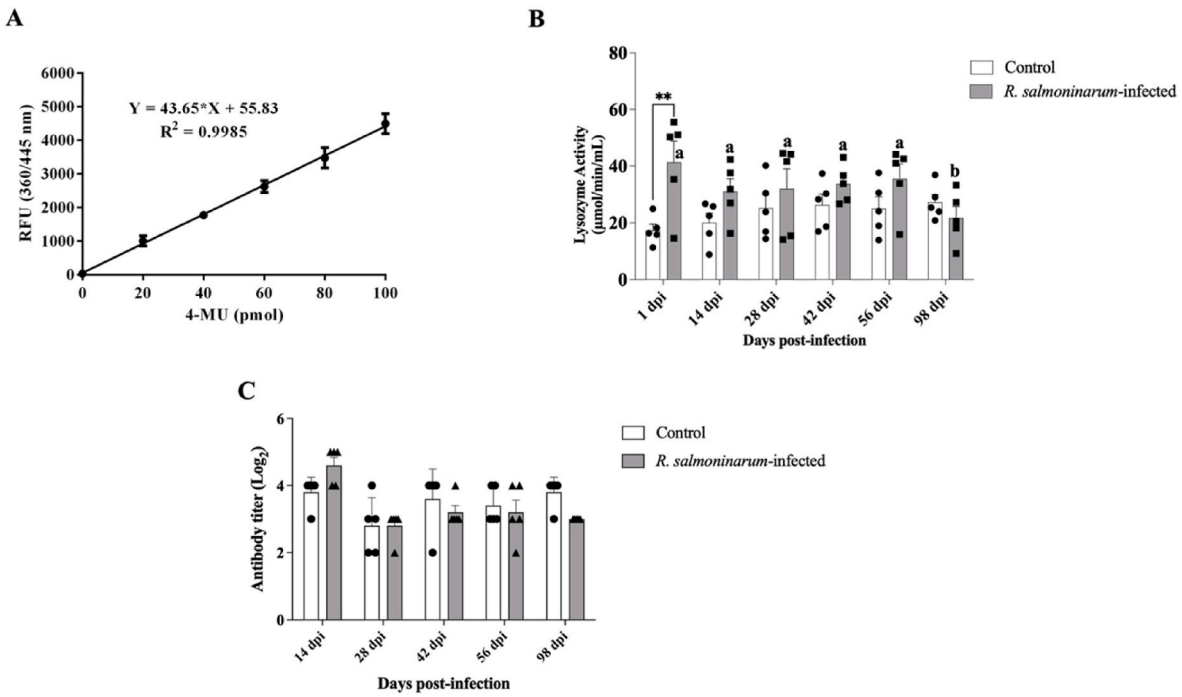

Fig. 6. Lysozyme activity and antibody titers in lumpfish serum upon *R. salmoninarum* infection. (**A**) Typical 4-Methylumbelliferon (4-MU) standard curve of the fluorometry-based lysozyme activity assay kit. (**B**) Lysozyme enzyme activity of control and *R. salmoninarum*-infected lumpfish serum at 1-, 14-, 28-, 42-, 56-, and 98-days post-infection from control and *R. salmoninarum*-infected (1×10^9 cells dose^{-1}) fish groups. A two-way ANOVA test, followed by the Sidak multiple comparisons post hoc test, was used to identify significant differences between treatments (control and infected groups) at a single time point and for a given treatment at different time points (1, 14, 28, 42, 56, and 98 dpi). Asterisks (*) represent significant differences between treatments at each time point (*$p < 0.05$, **$p < 0.01$). Lowercase letters represent significant differences between the lysozyme activity of the infected group at different time points. Each value is the mean ± S.E.M ($n = 5$). (**C**) *R. salmoninarum*-specific antibody levels were measured by indirect ELISA in lumpfish serum samples collected at 14-, 28-, 42-, 56-, and 98-dpi from control and *R. salmoninarum*-infected fish groups. Each value is the mean ± S.E.M ($n = 5$).

98 dpi (a total of 12 samples) used in the current RNA-seq analysis are the same ones we previously used in our qPCR study (Gnanagobal et al., 2021). Thus, to validate our current lumpfish head kidney transcriptome, we used the prior qPCR results from Gnanagobal et al. (2021) for 30 selected genes. The correlation analysis revealed that 83% of the qPCR-studied genes showed significant correlations ($R^2 \geq 0.5$) between qPCR and RNA-seq data (Fig. 5, Supplementary Fig. S2, and Supplementary Table S7). Therefore, in general, the qPCR and RNA-seq results were in high agreement, proving the reliability of the transcriptome data reported in this study. Our prior qPCR results also confirmed the induction of genes related to PRRs (e.g., *tlr5*), cytokines (e.g., *il1b, il8, il10*), iron homeostasis (e.g., *hamp*), and acute phase response (e.g., *saa5*) at 28 dpi, and cell-mediated adaptive immunity (e.g., *ifng, cd74*) at 98 dpi.

Innate immunity detects pathogens through a series of PRRs, which identify conserved pathogenic bacterial structures like flagellin and peptidoglycans and activate intracellular signalling pathways that result in inflammatory cytokines release and prime adaptive immunity. TLRs (Toll-like receptors), NLRs (NOD-like receptors), CLRs (C-type lectin receptors), and PGRP (peptidoglycan recognition proteins) are the 4 main types of PRRs found in fish (Gnanagobal and Santander, 2022). TLR5 is present in fish both in a membrane-bound (TLR5m) and soluble (TLR5s) forms and detects bacterial flagellin (Pietretti and Wiegertjes, 2014). Through TLR5m, flagellin first induce the basal activation of NFkB and promote TLR5s synthesis. Then, in a positive feedback loop, the TLR5s increases the cellular responses mediated by the TLR5m (Tsujita et al., 2004). *tlr5* was upregulated in the lumpfish head kidney in response to *R. salmoninarum* infection at 28 dpi, which is also verified by qPCR (Table 1, Fig. 5) (Gnanagobal et al., 2021). Although TLR5 induction by a non-motile or non-flagellated Gram-positive *R. salmoninarum* (Fryer and Sanders, 1981) is controversial, similar observations in TLR5 expression in response to *R. salmoninarum* and another non-motile Gram-positive pathogen, *Streptococcus iniae* were also reported in Atlantic salmon and turbot (*Scophthalmus maximus*), respectively (Eslamloo et al., 2020a, 2020b; Liu et al., 2017). Functional analyses are therefore required to understand the cross-talks between fish TLR5 and non-motile Gram-positive pathogens.

CLRs, which are calcium-dependent lectins that bind to carbohydrates (i.e., glycan structures of the pathogen), can activate several immune signalling pathways and have been implicated in complement activation, phagocytosis, cell death, inflammation, and antibacterial activities (da Silva Lino et al., 2014). *clec4e* (*si:ch73-86n18.1*; *C-type lectin domain family 4 member E*) showed upregulation in the lumpfish head kidney at 28 dpi (Table 1). In contrast, Eslamloo et al. (2020) observed variable expression of the C-type lectin family domain (i.e., upregulation of *clec12b* and downregulation of *clec3a* and *clec4e*) in response to *R. salmoninarum* bacterin in Atlantic salmon head kidney (Eslamloo et al., 2020b). Thus, C-type lectin family receptor induction in response to *R. salmoninarum* infection could be host-specific and vary between fish species. Little is known about CLR function in teleost fish, and the role of CLRs in lumpfish upon bacterial infection should be further explored at the gene or protein level to validate its variable expression between fish species.

PGRPs recognize the peptidoglycans (PGN) of the bacterial cell wall (i.e., binds strongly to murein PGN of Gram-positive bacteria) and kill Gram-positive pathogens by targeting their PGN biosynthesis (Kang et al., 1998). PGRPs demonstrated bactericidal activity in zebrafish (*Danio rerio*) and rockfish (*Sebastes schlegeli*) (Kim et al., 2010; Li et al., 2007). Gram-positive *R. salmoninarum* induced the expression of *pglyrp6* (*Peptidoglycan recognition protein 6*) in lumpfish at 28 dpi (Table 1). Similarly, Gram-positive *S. iniae* upregulated the PGRP gene (*Smpgrp2*) in mucosal tissues of turbot following challenge (Zhang et al., 2016).

PGRP's involvement in intracellular immune signalling and lumpfish host defense is unknown and warrants future research.

Complement systems and antibodies, which identify and eliminate invading pathogens and stimulate inflammation, are the key humoral elements of innate immunity (Nakao et al., 2011). *R. salmoninarum* is known to activate the alternative complement pathway, where opsonin C3b directly binds to the bacterial surface and facilitates the intracellular invasion of bacteria into fish phagocytes (Gnanagobal and Santander, 2022; Rose and Levine, 1992). Similarly, our RNA-seq results indicated that *R. salmoninarum* activates alternative complement cascading and relevant genes, including complement C3-like gene (*LOC117745115*), at 28 dpi in lumpfish (Table 1; Supplementary Table S5). Complement activation in lumpfish was also reported against Gram-negative pathogens, *V. anguillarum* and *A. salmonicida* (Chakraborty et al., 2022; Eggestøl et al., 2018).

Nutritional immunity is a defense response against invading pathogens, where the host deprives the intracellular availability of critical nutrients, including iron, and amino acids, to limit bacterial proliferation (Abu Kwaik and Bumann, 2013; Barel and Charbit, 2013; Hood and Skaar, 2012). Hepcidin (HAMP), a major iron metabolism regulator, is increased as a result of interleukin 6 (IL-6)-mediated hypoferric inflammatory response, which in turn inhibits iron exporters (i.e., ferroportin) and lowers the iron in tissues to a level below which the pathogen cannot proliferate and cause disease (Gnanagobal and Santander, 2022; Nemeth and Ganz, 2006). Teleost HAMP also presents antibacterial activity against Gram-positive bacteria (Cai et al., 2012; Neves et al., 2017). In the present study, lumpfish significantly upregulated several hepcidin or hepcidin-like genes (i.e., *hamp*, *LOC117728128*, and *LOC117728096*) in response to *R. salmoninarum* at 28 dpi. As in the RNA-seq results, our prior qPCR also showed statistically significant upregulation of *hamp* with a similar fold change (Gnanagobal et al., 2021) (Table 1 and Supplementary Table S3) and a significant correlation between TPM and RQ values (Fig. 5). Similar to what we found in lumpfish, elevated expression levels of *hamp* were seen in other fish species in response to Gram-positive pathogens at early infection stages. These other fish species were Atlantic salmon (head kidney) following *R. salmoninarum* infection (Eslamloo et al., 2020a, 2020b), hybrid striped bass (*Morone chrysops* × *Morone saxatilis*; liver) against *S. iniae* (Lauth et al., 2005), and European sea bass (*Dicentrarchus labrax*; liver) following *Lactococcus garviae* and *Streptococcus parauberis* infection (Neves et al., 2017). As lumpfish seem to have multiple hepcidin or hepcidin-like genes (Supplementary Table S3), future research on their structural and functional characterization and their involvement in the lumpfish antibacterial responses would be valuable.

Beyond the canonical lumpfish host immune-related response, we observed substantial dysregulation of the processes associated with amino acid metabolism; in particular, lumpfish downregulated genes involved in amino acid biosynthesis and degradation during the *R. salmoninarum* infection at 28 dpi (Table 1; Supplementary Table S6). Similar findings were also reported in Atlantic salmon in response to *R. salmoninarum* and another intracellular pathogen, *P. salmonis* (Eslamloo et al., 2020a; Valenzuela-Miranda and Gallardo-Escárate, 2018). For instance, Eslamloo et al. (2020a) observed extensive metabolic dysregulation of protein-related processes, including amino acid activation and cellular amino acid metabolism, in the Atlantic salmon head kidney upon *R. salmoninarum* infection at 13 dpi. Both the Atlantic salmon (head kidney and spleen) and *P. salmonis* showed a greater number of genes related to the amino acid metabolism when host and pathogen transcriptomes were analyzed simultaneously (Valenzuela--Miranda and Gallardo-Escárate, 2018). The authors also discovered that *P. salmonis* lacks certain amino acid biosynthesis pathways (e.g., valine, leucine, and isoleucine) and, therefore, is metabolically dependent on the amino acids present in its salmon host during infection (Valenzuela-Miranda and Gallardo-Escárate, 2018). According to Wiens et al. (2008), the *R. salmoninarum* type strain, which we used in the present study, lacks *de novo* biosynthesis of the amino acids serine, glycine, cysteine, asparagine, and methionine (Wiens et al., 2008). Intriguingly, the amino acid metabolism-related processes were downregulated in lumpfish upon *R. salmoninarum* infection at 28 dpi, including biosynthesis of glycine, serine, aspartate, cellular amino acids, and sulfur amino acids (i.e., cysteine and methionine) (Table 1; Supplementary Table S6). Therefore, like *P. salmonis*, *R. salmoninarum* may rely on the fish host's intracellular environment to uptake amino acids that its own cell machinery cannot synthesize. As a defense response, lumpfish potentially downregulated processes or genes related to amino acid biosynthesis and import to limit the availability of amino acids in fish tissues. Although amino acid metabolism is not a predominant transcriptome response in lumpfish in the current RNA-seq study, this scenario could be seen in the context of amino acid-based nutritional immunity induced by lumpfish to overcome *R. salmoninarum* during early infection stages. Research on how intracellular *R. salmoninarum* overcomes amino acid starvation within the host (i.e., nutritional virulence) or how it uses the host machinery to get amino acids from the host cell would be intriguing. Further, future *in-vitro* assays will be required to confirm the role of the critical amino acids in *R. salmoninarum* growth and metabolism.

Apoptosis or programmed cell death is a crucial defense mechanism against pathogens (Miller, 1997). Caspase-associated recruitment domain (CARD) regulates caspase activation during apoptosis and inflammation and NFkB activation during innate or adaptive immunity (Bouchier-Hayes and Martin, 2002). A positive regulator of apoptosis and NFkB activation, B cell lymphoma (BCL) 10 is an adaptor protein containing a CARD (Lucas et al., 2001). Association between CARDs from CARD-family proteins and B cell lymphoma 10 activates the NFkB pathway (Bhatt and Ghosh, 2014; Dubois et al., 2014). In teleost fish, genes for CARD-containing proteins implicated in NFkB activation have been identified (Chang et al., 2010; Kono et al., 2003). According to our RNA-seq results, induction of genes *card9*, *bcl3,* and *LOC117734930* in response to *R. salmoninarum* infection at 28 dpi suggests the activation of apoptosis and NFkB signalling pathways in lumpfish (Table 1). This might be how lumpfish facilitate the apoptotic clearance of infected cells. Further, Atlantic salmon also exhibited an abundance of BPs linked to cell death and increased expression of apoptotic caspase (*casp14*) against *R. salmoninarum* infection (Eslamloo et al., 2020a). Studies on the structural and functional characterization of the lumpfish *card9* gene and examining its role in immune modulation would be interesting since it may be a promising biomarker for infection.

The JAK-STAT signalling pathway plays crucial roles in immune system orchestration, especially in mediating immune regulatory processes (Seif et al., 2017). In mammals, a canonical JAK-STAT pathway is activated when the receptor binds to the ligand and deactivated when negative regulators are present (Seif et al., 2017). Cytokines (i.e., ligands) IL-6, a pro-inflammatory cytokine, and IL-10, an anti-inflammatory cytokine, bind to their receptor, glycoprotein 130 (Gp130) and IL-10 receptor, respectively, and the ligand/receptor complex activates the JAK-STAT signalling cascade (Carey et al., 2012; Lokau et al., 2019; Seif et al., 2017). Suppressors of cytokine signalling (SOCS) and cytokine-inducible SH2 (Src homology 2) domain protein (CISH) are the negative regulators that function to inhibit JAK-STAT signalling (Seif et al., 2017). Several signalling molecules, including PI3 kinase (PI3K), MAPK, and ERK, participate in this pathway (Seif et al., 2017). RNA-seq results presented in this study show that JAK-STAT signalling was found to be dysregulated by *R. salmoninarum* in lumpfish head kidney at 28 dpi, similar to what was reported in Atlantic salmon head kidney transcriptome profiling in response to this pathogen (Eslamloo et al., 2020a). Thus, the JAK-STAT pathway may play a crucial role in the host-pathogen interactions between *R. salmoninarum* and lumpfish during early infection stages. To be specific, *R. salmoninarum* infection upregulated genes linked to JAK-STAT signalling (Table 1). For instance, the ligands *interleukin-6-like* (*LOC117739248*) and *interleukin-10* (*il10*) were upregulated (Table 1; Supplementary Table 5). Significant pathogen-responsive induction of

il10 was also verified by qPCR (Fig. 5). Interestingly, *R. salmoninarum* infection at 28 dpi also caused upregulation of the receptor, *il10 receptor subunit beta-like* (*LOC117750018*) and negative regulators, *socs3a*, and *cish*, suggesting the IL-10 mediated signal transduction (i.e., IL-10-JAK-STAT-Circuit), and suppression of JAK-STAT signalling, respectively. Inhibition of the JAK-STAT signalling pathway could be seen from both the host and the pathogen points of view. From the lumpfish point of view, the infection-induced IL-10-JAK-STAT module may balance the pro-inflammatory responses and prevent host-mediated immune hyperactivity (Carey et al., 2012). But, from the pathogen perspective, *R. salmoninarum* may hijack the JAK-STAT module through IL-10, SOCS, and CISH upregulation to sabotage host immune responses and promote its intracellular survival (Carey et al., 2012). It is important to note that the RNA-seq results presented herein only give an overview of up- and down-regulated genes in response to *R. salmoninarum* infection in lumpfish based on pathway enrichment analyses and offer speculations using the significantly dysregulated genes but do not reveal the exact mechanisms of immune modulation. Thus, future studies are required to validate the lumpfish JAK-STAT signalling pathway and to functionally characterize the genes involved in this mechanism.

In teleost fish, cell-mediated adaptive immunity involves $CD8^+$ T cells to kill intracellular pathogens (Munang'andu, 2018). As MHC-1 molecules present processed intracellular antigens to $CD8^+$ T cells, they become cytotoxic T lymphocytes and release cytotoxic granules that cause infected cells to undergo apoptosis. Cytokines, such as IFN-γ, trigger $CD4^+$ T cells to differentiate into T helper 1 (Th1) cells, which prime $CD8^+$ cells (Gnanagobal and Santander, 2022; Munang'andu, 2018). At 28 dpi, a Th1-type immune response was seen, along with the upregulation of *tap2a*, which is linked to MHC-1-mediated antigen processing and presentation (Table 1 and Supplementary Table S5). Subsequently, at 98 dpi, genes related to T-cell mediated cytotoxicity and the MHC-1 pathway were stimulated. Eslamloo et al. (2020a) also noted interactions between *R. salmoninarum* and the MHC-1 pathway in Atlantic salmon, which is similar to what we saw in lumpfish. Infected lumpfish were dying at the early stage, but mortality was stabilized with persisted *R. salmoninarum* at the chronic infection stage (Fig. 1B). Thus, *R. salmoninarum* may evade (i.e., escape into the cytosol from the phagosome) the MHC-1 antigen presentation pathway during early infection, while lumpfish survived chronic infection by limiting *R. salmoninarum* growth with induced cell-mediated immunity. Future studies are needed to understand how *R. salmoninarum* evades antigen presentation pathways or interacts with the MHC-1 pathway in teleosts.

A crucial indicator of fish innate immunity is lysozyme activity (Bayne and Gerwick, 2001). Fish lysozyme is lytic against Gram-positive and Gram-negative bacteria (Saurabh and Sahoo, 2008). It is present in mucus, serum, lymphoid tissues, and phagocytic cells of marine and freshwater fish (Saurabh and Sahoo, 2008). Since fish appear to have a less developed specific immune system than mammals, non-specific antimicrobial compounds like lysozyme may be more significant in fish than in mammals (Grinde et al., 1988). Besides having bactericidal properties, lysozyme is opsonic and thus activates the complement pathway and phagocytes (Saurabh and Sahoo, 2008). Increased levels of lysozyme at the first sampling point (1 dpi) were followed by no significant difference between infected and time-matched control samples at subsequent time points (14, 28, 42, 56, and 98 dpi) in the serum from *R. salmoninarum*-infected lumpfish compared to the control fish (Fig. 6B). These findings corroborate those made in carp (*Cyprinus carpio*) infected with Gram-negative *Pseudomonas alcaligenes* and *Aeromonas punctata* or tilapia (*Oreochromis niloticus*) infected with Gram-positive *Streptococcus agalactiae* (Biller et al., 2021; Siwicki and Studnicka, 1987). Pathogen recognition initiates a rapid innate immune response, including lysozyme activity, and subsequently induces host immunity via multiple signalling pathways and defense mechanisms (Janeway and Medzhitov, 2002). Therefore, earlier samplings, such as a few hours to a day after the challenge, may find elevated lysozyme levels. On the other hand, reduction in serum lysozyme activity at later time points means that the adaptive response or further defense mechanisms have been given the opportunity to take over (Biller et al., 2021).

An understanding of the humoral immune response elicited against bacterial infection can be gained by measuring the antibody titers in the serum of infected fish using ELISA. At all of the time points, no significant variations in $\log_2$ antibody titers between control and infected fish serum were seen (Fig. 6C), indicating that either the circulating antibody levels in lumpfish may not considerably impacted by *R. salmoninarum* infection or lumpfish may induced a poor specific antibody response to infection. This could be due to the immune suppressive protein p57 of *R. salmoninarum* adsorbing specific antibodies and forming antigen-antibody complexes or opsonization of such complexes (Fredriksen et al., 1997; Kaattari and Piganelli, 1997; Rømer Villumsen et al., 2012; Turaga et al., 1987). In contrast, elevated levels of BKD-induced serum antibody titers were observed in Atlantic salmon and rainbow trout (*Oncorhynchus mykiss*) (Jansson and Ljungberg, 1998). Thus, specific antibody response to this pathogen may have varied between fish species.

It has been demonstrated that the antibody levels in several fish species, including Atlantic lumpfish, may decrease in lower water temperatures and increase in higher water temperatures (Erkinharju et al., 2018; Makrinos and Bowden, 2016). Also, specific immune responses, such as antibody production or upregulation of antibody-related functions, were greater at higher temperatures (Alcorn et al., 2002; Makrinos and Bowden, 2016; Rozas-Serri et al., 2020). In a multi-year study of sockeye salmon reared at 8 °C or 12 °C for their entire life cycle, fish at 12 °C produced greater antigen-specific serum antibody levels than those at 8 °C to recombinant p57 protein of *R. salmoninarum* (Alcorn et al., 2002). Humoral response-related transcripts, IgM and IgT, were overexpressed in *R. salmoninarum* infected fish (Atlantic salmon pre-smolts head kidney) at 15 °C compared to those at 11 °C (Rozas-Serri et al., 2020). Further, in a study analyzing the effect of temperature on the immunization of Atlantic lumpfish with *Aeromonas salmonicida* antigens, vaccinated fish kept at both 10 °C and 12 °C showed higher antibody (IgM) responses than the fish at low temperature (5 °C) (Erkinharju et al., 2018). Lumpfish were kept at 8–10 °C in our study. It is possible that lumpfish may not have responded well to *R. salmoninarum* at low temperatures (8–10 °C) in terms of antibody response. Given the above interactions between high temperatures and antibody response, keeping lumpfish at higher temperatures, such as 12–15 °C, may result in increased antibody levels in response to *R. salmoninarum*.

Fig. 7 illustrates the putative immune pathways activated by *R. salmoninarum* infection in the lumpfish head kidney. Although *R. salmoninarum* infection affected many genes and pathways, particularly at 28 dpi, only a small percentage of them were associated with the immune response (7%) compared to the cellular (63%) and metabolic (25%) processes in the global view (Fig. 3A), suggesting that this pathogen may have suppressed the lumpfish immune system during the early stages of infection. As per RNA-seq and qPCR results, simultaneous upregulation of genes encoding canonical pro- and anti-inflammatory cytokines (*il1b, il8*, *il10*), downregulation of innate immunity activation (*inavaa*), negative regulation of BPs connected to adaptive immunity (i.e., negative regulation of interferon-gamma production, immune effector process, T cell activation/differentiation) and inhibition of JAK-STAT signalling (*socs3a*, and *cish*) also point to *R. salmoninarum*-induced immune suppression at the early infection stage (Fig. 7A). On the other hand, at 98 dpi, lumpfish induced cell-mediated immunity related to the MHC-1 pathway suggests that *R. salmoninarum* may be present in the cytoplasm during intracellular infection.

Our transcriptomics results provide valuable baseline information regarding the biological processes and molecular pathways underlying the lumpfish response to a Gram-positive fish pathogen, *R. salmoninarum,* during the early and chronic infection stages (Fig. 7B). Knowledge of immune genes or pathways dysregulated in lumpfish during *R. salmoninarum* infection from the present study will be valuable

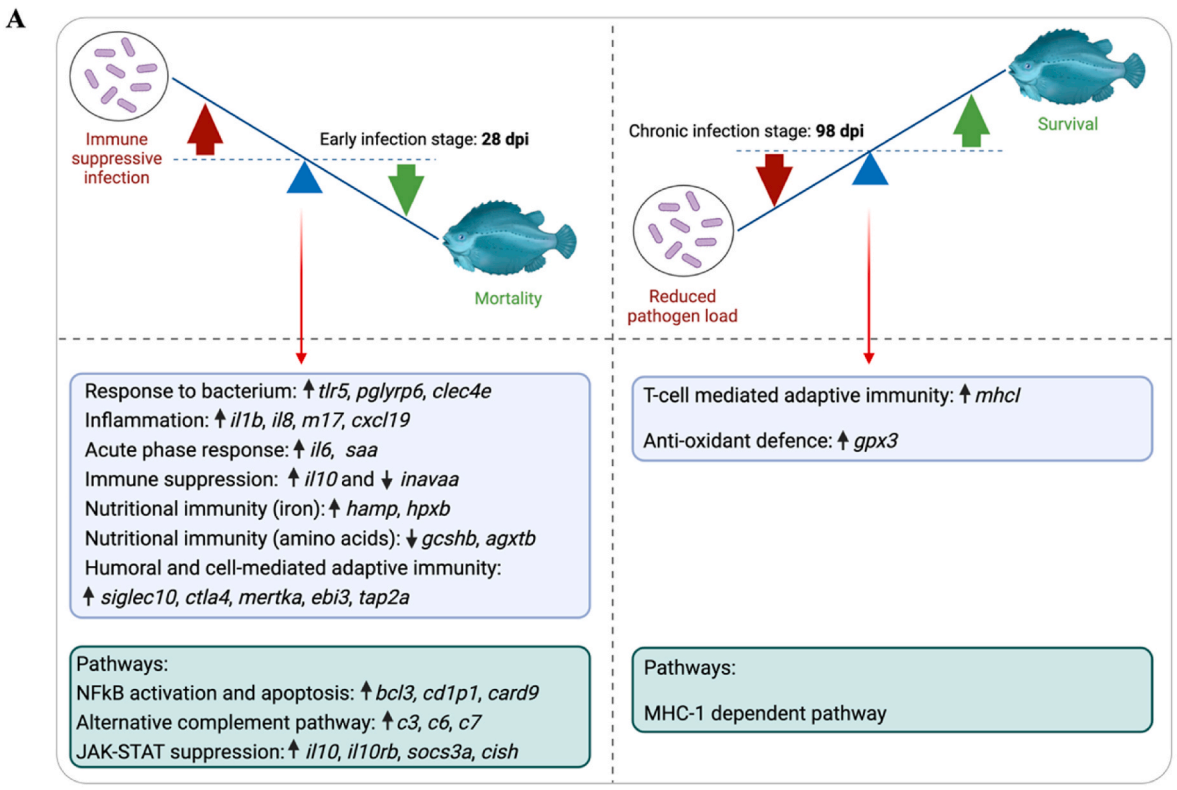

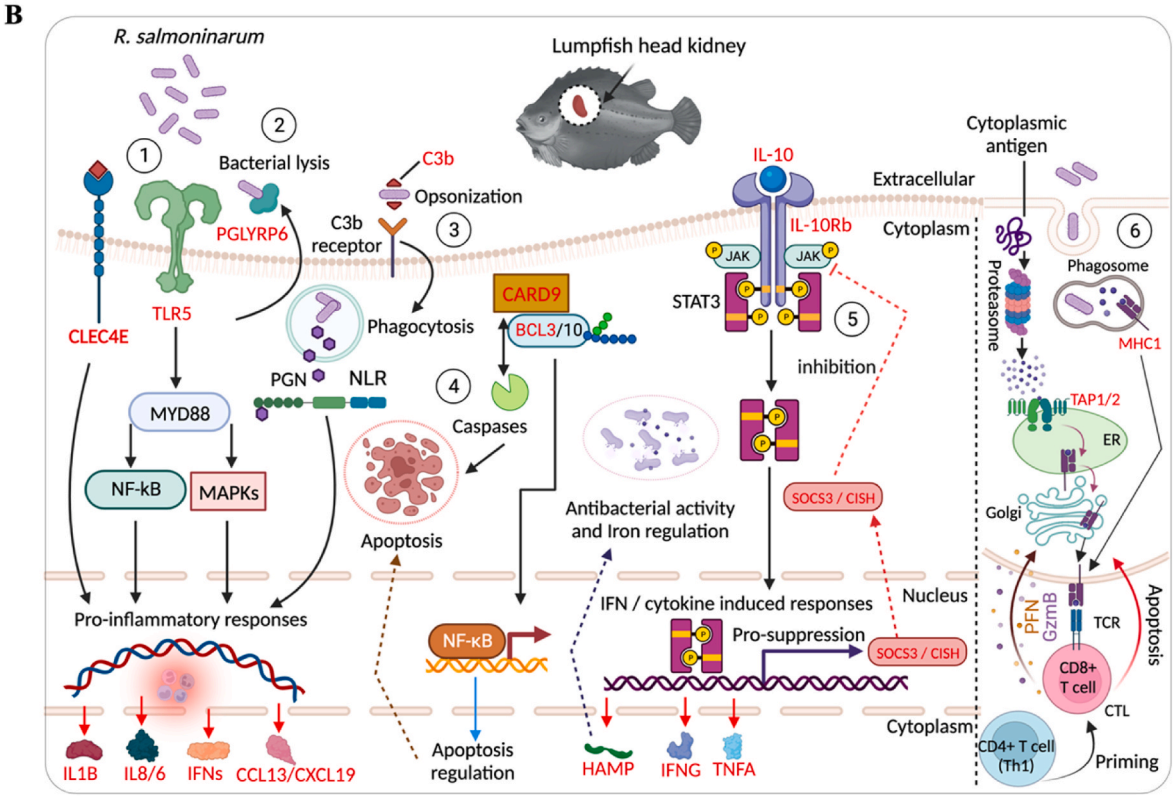

(caption on next page)

Fig. 7. Lumpfish head kidney transcriptome response to *R. salmoninarum* at early (28 dpi) and chronic (98 dpi) infection stages. (**A**) Immune genes and pathways dysregulated in lumpfish at 28 and 98 dpi. At earlier stages of infection (i.e., the onset of mortality), immune suppressive infection by *R. salmoninarum* caused mortality in lumpfish (i.e., *R. salmoninarum* took over the tug-of-war at 28 dpi). On the other hand, lumpfish survived at chronic stages of infection with induced cell-mediated immunity (i.e., lumpfish took over the tug-of-war at 98 dpi). and indicate up- and down-regulation of the genes, respectively (Table 1). (**B**) Schematic representation of the host molecular pathways differentially regulated by *R. salmoninarum* in lumpfish. This figure was created using the genes found in this study (red fonts) and their regulatory pathways and functions in mammals, as described in the Discussion. **1.** TLR-mediated signalling and NFkB activation. **2.** Secreted peptidoglycan recognition proteins (PGLYRPs) interact with the bacterial peptidoglycan (PGN) and induce bacterial lysis. **3.** Complement pathway - C3b binding to the bacterial surface, followed by ligation to the C3b receptor and bacterial internalization by phagocytosis. Following degradation in the phagolysosome, PGN-derived small molecules are sensed by NOD-like receptors (NLRs) to induce pro-inflammatory cytokines. **4.** Apoptosis and NFkB activation through interactions between Caspase-associated recruitment domain (CARD) family proteins and B-cell lymphoma adaptor proteins (BCL3/10). **5.** JAK-STAT signalling (IL-10-JAK-STAT-Circuit) and its negative regulation (red-dotted arrows) by suppressors of cytokine signalling (SOCS) and cytokine-inducible SH2 domain protein (CISH). **6.** Interactions with the MHC-I dependent pathway. MHC-I molecules present processed intracellular antigens to $CD8^+$ T cells. These $CD8^+$ T cells become cytotoxic T-lymphocytes (CTL) and release perforins (PFN; form pores in the plasma membrane) and granzymes (GZm; break down proteins and lyse the cells) into the infected cells and kill them. $CD4^+$ T cells help $CD8^+$ T cells priming to kill the intracellular pathogen. TLR, Toll-like receptor; MyD88, Myeloid differentiation primary response 88; NFkB, Nuclear factor kappa-B; MAPK, Mitogen-activated protein kinase; ILs, interleukin; IFNs, Interferons; CCL13, C–C motif chemokine; CXCL19, C-X-C motif chemokine 19; PGN, Peptidoglycans; PGLYRP6, Peptidoglycan recognition protein 6; NLR, NOD-like receptors; CLEC4E, C-type lectin domain family 4 member E; C3b, Complement B; CARD, Caspase-associated recruitment domain; BCL3, B-cell lymphoma 3; IL-10Rb, Interleukin-10 receptor subunit beta-like; JAK, Janus kinase; P, Phosphorylation; STAT, Signal transducer and activator of transcription; SOCS, Suppressors of cytokine signalling; CISH, Cytokine-inducible SH2 (Src homology 2) domain protein; HAMP, Hepcidin antimicrobial peptide; IFNG, Interferon gamma; TNFA, Tumor necrosis factor alpha; MHC1, Major histocompatibility complex I; TAP, Protein associated with antigen processing; ER, Endoplasmic reticulum protein; PFN, Perforin; GZm, Granzyme; TCR, T-cell receptor; CD, Cluster of differentiation; CTL, Cytotoxic T-lymphocytes. Figures A and B were created in BioRender (https://biorender.com/). (For interpretation of the references to color in this figure legend, the reader is referred to the Web version of this article.)

for immuno-prophylaxis. For instance, vaccine design with pertinent intracellular antigens that target cell-mediated immunity ($CD8^+$ T-cells), and MHC-1 antigen presentation pathway may induce protection against this intracellular pathogen. Future RNA-seq analyses that simultaneously compare the transcriptomes of salmon and lumpfish in a cohabitation *R. salmoninarum* infection model would be beneficial to identify comparative molecular biomarkers for BKD-related investigations. Furthermore, to improve our existing understanding of the lumpfish immune system, it is crucial to characterize the functions of the important immune-relevant genes identified herein.

5. Conclusion

A global overview of the molecular mechanisms underlying lumpfish responses to *R. salmoninarum* during early (28 dpi) and chronic (98 dpi) infection stages was provided by this study, which used RNA-seq to profile the lumpfish head kidney transcriptome. Compared to 98 dpi, *R. salmoninarum* affected greater numbers of pathways and genes in lumpfish at 28 dpi. However, only a small percentage of them were related to immune responses, which might be attributed to the immune suppressive nature of this pathogen. At 28 dpi, *R. salmoninarum*-induced genes were linked to innate and adaptive immunity, and the pathways that were dysregulated include NFkB signaling, apoptosis, alternative complement cascading, and JAK-STAT signaling pathway. *R. salmoninarum*-suppressed genes in lumpfish at 28 dpi were associated with cellular and metabolic processes (e.g., amino acid biosynthesis/degradation). Lumpfish triggered MHC-1-related cell-mediated immunity against *R. salmoninarum* at 98 dpi, linked to its cytoplasmic location during intracellular infection. Lysozyme activity in infected lumpfish serum was higher at the earliest time point (1 dpi) and subsequently reduced at later time points (14, 28, 42, 56, and 98 dpi). *R. salmoninarum* infection did not significantly affect the antibody titers in lumpfish, according to ELISA. Overall, the present study is a combined approach of reference-based transcriptomic assembly and pathway enrichment analyses that provided gene repertoires and networks that regulate the host-pathogen interactions between lumpfish and *R. salmoninarum* and will act as a guide to understand host immunity and pathogen virulence.

Funding

This work was funded through a grant from MUN Seed, Bridge, and Multidisciplinary Funds; NSERC-Discovery (RGPIN-2018-05942); Research and Development Corporation (RDC) of Newfoundland and Labrador, R&D-Ignite Project #5404.2113.10; and Ocean Frontier Institute, Canada First Research Excellence Fund (Module J.3) and Ocean Frontier Institute, Vitamin Funds.

CRediT authorship contribution statement

Hajarooba Gnanagobal: Conceptualization, Data curation, Formal analysis, Investigation, Methodology, Project administration, Software, Validation, Visualization, Writing – original draft, Writing – review & editing. **Setu Chakraborty:** Data curation, Investigation, Methodology, Writing – review & editing. **Ignacio Vasquez:** Investigation, Methodology, Writing – review & editing. **Joy Chukwu-Osazuwa:** Investigation, Methodology, Writing – review & editing. **Trung Cao:** Investigation, Methodology, Writing – review & editing. **Ahmed Hossain:** Investigation, Methodology, Writing – review & editing. **My Dang:** Investigation, Methodology, Writing – review & editing. **Katherine Valderrama:** Investigation, Methodology, Writing – review & editing. **Surendra Kumar:** Investigation, Methodology, Software, Writing – review & editing. **Gabriela Bindea:** Investigation, Methodology, Software, Visualization, Writing – review & editing. **Stephen Hill:** Investigation, Methodology, Writing – review & editing. **Danny Boyce:** Funding acquisition, Resources, Writing – review & editing. **Jennifer R. Hall:** Data curation, Investigation, Methodology, Software, Writing – review & editing. **Javier Santander:** Conceptualization, Data curation, Formal analysis, Funding acquisition, Investigation, Methodology, Resources, Software, Supervision, Validation, Visualization, Writing – original draft, Writing – review & editing.

Declaration of competing interest

The authors declare no competing interests.

Data availability

RNA-seq raw data of the current study are available in NCBI Sequence Read Archive (SRA) database under the bioproject accession number PRJNA978536.

Acknowledgments

The authors are thankful to Dr. Matthew Rise (Department of Ocean Sciences, MUN) and Dr. Víctor Antonio García-Angulo (Institute of Biomedical Sciences, Facultad de Medicina, Universidad de Chile, Santiago, Chile) for their valuable feedback on the manuscript and to the Dr. Joe Brown Aquatic Research Building (JBARB) staff and the Cold-Ocean

Deep-Sea Research Facility (CDRF) staff for their assistance with the fish assays.

Appendix A. Supplementary data

Supplementary data to this article can be found online at https://doi.org/10.1016/j.dci.2024.105165.

References

Abu Kwaik, Y., Bumann, D., 2013. Microbial quest for food in vivo: "Nutritional virulence" as an emerging paradigm. Cell Microbiol. 15, 882–890. https://doi.org/10.1111/cmi.12138.

Alcorn, S.W., Murray, A.L., Pascho, R.J., 2002. Effects of rearing temperature on immune functions in sockeye salmon (*Oncorhynchus nerka*). Fish Shellfish Immunol. 12, 303–334. https://doi.org/10.1006/fsim.2001.0373.

Barel, M., Charbit, A., 2013. *Francisella tularensis* intracellular survival: to eat or to die. Microb. Infect. 15, 989–997. https://doi.org/10.1016/j.micinf.2013.09.009.

Bayne, C.J., Gerwick, L., 2001. The acute phase response and innate immunity of fish. Dev. Comp. Immunol. 25, 725–743. https://doi.org/10.1016/S0145-305X(01)00033-7.

Bhatt, D., Ghosh, S., 2014. Regulation of the NF-κB-mediated transcription of inflammatory genes. Front. Immunol. 5, 71.

Biller, J.D., Polycarpo, G. do V., Moromizato, B.S., Sidekerskis, A.P.D., Silva, T.D. da, Reis, I.C. dos, Fierro-Castro, C., 2021. Lysozyme activity as an indicator of innate immunity of tilapia (*Oreochromis niloticus*) when challenged with LPS and *Streptococcus agalactiae*. Rev. Bras. Zootec. 50.

Bindea, G., Mlecnik, B., Hackl, H., Charoentong, P., Tosolini, M., Kirilovsky, A., Fridman, W.-H., Pagès, F., Trajanoski, Z., Galon, J., 2009. ClueGO: a Cytoscape plug-in to decipher functionally grouped gene ontology and pathway annotation networks. Bioinformatics 25, 1091–1093. https://doi.org/10.1093/bioinformatics/btp101.

Boissonnot, L., Kharlova, I., Iversen, N.S., Staven, F.R., Austad, M., 2022. Characteristics of lumpfish (*Cyclopterus lumpus*) with high cleaning efficacy in commercial Atlantic salmon (Salmo salar) production. Aquaculture 560, 738544. https://doi.org/10.1016/j.aquaculture.2022.738544.

Bouchier-Hayes, L., Martin, S.J., 2002. CARD games in apoptosis and immunity. EMBO Rep. 3, 616–621.

Brooker, A.J., Papadopoulou, A., Gutierrez, C., Rey, S., Davie, A., Migaud, H., 2018. Sustainable production and use of cleaner fish for the biological control of sea lice: recent advances and current challenges. Vet. Rec. 183, 383.

Byford, G.J., Faisal, M., Tempelman, R.J., Scribner, K.T., 2020. Prevalence and distribution of *Renibacterium salmoninarum* in non-salmonid fishes from Laurentian Great Lakes and inland habitats. J. Great Lake. Res. 46, 1709–1715. https://doi.org/10.1016/j.jglr.2020.09.014.

Cai, L., Cai, J.J., Liu, H.P., Fan, D.Q., Peng, H., Wang, K.J., 2012. Recombinant medaka (*Oryzias melastigmus*) pro-hepcidin: Multifunctional characterization. Comp. Biochem. Physiol. B Biochem. Mol. Biol. 161, 140–147. https://doi.org/10.1016/j.cbpb.2011.10.006.

Carey, A.J., Tan, C.K., Ulett, G.C., 2012. Infection-induced IL-10 and JAK-STAT. JAK-STAT 1, 159–167. https://doi.org/10.4161/jkst.19918.

Chakraborty, S., Hossain, A., Cao, T., Gnanagobal, H., Segovia, C., Hill, S., Monk, J., Porter, J., Boyce, D., Hall, J.R., Bindea, G., Kumar, S., Santander, J., 2022. Multi-organ transcriptome response of lumpfish (*Cyclopterus lumpus*) to *Aeromonas salmonicida* subspecies *salmonicida* systemic infection. Microorganisms. https://doi.org/10.3390/microorganisms10112113.

Chang, M.X., Chen, W.Q., Nie, P., 2010. Structure and expression pattern of teleost caspase recruitment domain (CARD) containing proteins that are potentially involved in NF-kappaB signalling. Dev. Comp. Immunol. 34, 1–13. https://doi.org/10.1016/j.dci.2009.08.002.

Cohen, J., 1968. Weighted kappa: nominal scale agreement with provision for scaled disagreement or partial credit. Psychol. Bull. 70, 213–220. https://doi.org/10.1037/h0026256.

Crowther, J.R., 2000. The ELISA guidebook. Methods Mol. Biol. 149 (III–IV), 1–413. https://doi.org/10.1385/1592590497.

da Silva Lino, M.A., Bezerra, R.F., da Silva, C.D.C., Carvalho, E., Coelho, L., 2014. Fish lectins: a brief review. Adv. Zool. Res. Nov. Sci. Hauppauge 95–114.

Dang, M., Cao, T., Vasquez, I., Hossain, A., Gnanagobal, H., Kumar, S., Hall, J.R., Monk, J., Boyce, D., Westcott, J., Santander, J., 2021. Oral immunization of larvae and juvenile of lumpfish (*Cyclopterus lumpus*) against *Vibrio anguillarum* does not influence systemic immunity. Vaccines 9, 819. https://doi.org/10.3390/vaccines9080819.

Dubois, S.M., Alexia, C., Wu, Y., Leclair, H.M., Leveau, C., Schol, E., Fest, T., Tarte, K., Chen, Z.J., Gavard, J., Bidère, N., 2014. A catalytic-independent role for the LUBAC in NF-κB activation upon antigen receptor engagement and in lymphoma cells. Blood 123, 2199–2203. https://doi.org/10.1182/blood-2013-05-504019.

Eggestøl, H.Ø., Lunde, H.S., Rønneseth, A., Fredman, D., Petersen, K., Mishra, C.K., Furmanek, T., Colquhoun, D.J., Wergeland, H.I., Haugland, G.T., 2018. Transcriptome-wide mapping of signaling pathways and early immune responses in lumpfish leukocytes upon in vitro bacterial exposure. Sci. Rep. 8, 5261. https://doi.org/10.1038/s41598-018-23667-x.

Eissa, A.E., Elsayed, E.E., McDonald, R., Faisal, M., 2006. First record of *Renibacterium salmoninarum* in the sea lamprey (*Petromyzon marinus*). J. Wildl. Dis. 42, 556–560. https://doi.org/10.7589/0090-3558-42.3.556.

Erkinharju, T., Dalmo, R.A.Vågsnes, Hordvik, I., Seternes, T., 2018. Vaccination of Atlantic lumpfish (*Cyclopterus lumpus* L.) at a low temperature leads to a low antibody response against *Aeromonas salmonicida*. J. Fish. Dis. 41, 613–623. https://doi.org/10.1111/jfd.12760.

Eslamloo, K., Caballero-Solares, A., Inkpen, S.M., Emam, M., Kumar, S., Bouniot, C., Avendaño-Herrera, R., Jakob, E., Rise, M.L., 2020a. Transcriptomic profiling of the adaptive and innate immune responses of atlantic salmon to *Renibacterium salmoninarum* infection. Front. Immunol. 11 https://doi.org/10.3389/fimmu.2020.567838.

Eslamloo, K., Kumar, S., Caballero-Solares, A., Gnanagobal, H., Santander, J., Rise, M.L., 2020b. Profiling the transcriptome response of Atlantic salmon head kidney to formalin-killed *Renibacterium salmoninarum*. Fish Shellfish Immunol. 98, 937–949. https://doi.org/10.1016/j.fsi.2019.11.057.

Evelyn, T., Prosperi-Porta, L., Ketcheson, J., 1990. Two new techniques for obtaining consistent results when growing *Renibacterium salmoninarum* on KDM2 culture medium. Dis. Aquat. Org. 9, 209–212. https://doi.org/10.3354/dao009209.

Evelyn, T.P., 1993. Bacterial kidney disease – BKD. In: V, Roberts, R.J., Bromage, N.R. (Eds.), Bacterial Disease of Fish. Blackwell Scientific, London, pp. 177–195.

Everaert, C., Luypaert, M., Maag, J.L.V., Cheng, Q.X., Dinger, M.E., Hellemans, J., Mestdagh, P., 2017. Benchmarking of RNA-sequencing analysis workflows using whole-transcriptome RT-qPCR expression data. Sci. Rep. 7, 1559.

Ewels, P., Magnusson, M., Lundin, S., Käller, M., 2016. MultiQC: summarize analysis results for multiple tools and samples in a single report. Bioinformatics 32, 3047–3048. https://doi.org/10.1093/bioinformatics/btw354.

Fredriksen, Å., Endresen, C., Wergeland, H.I., 1997. Immunosuppressive effect of a low molecular weight surface protein from *Renibacterium salmoninarum* on lymphocytes from Atlantic salmon (*Salmo salar* L.). Fish Shellfish Immunol. 7, 273–282. https://doi.org/10.1006/fsim.1997.0082.

Fryer, J.L., Sanders, J.E., 1981. Bacterial kidney disease of salmonid fish. Annu. Rev. Microbiol. 35, 273–298. https://doi.org/10.1146/annurev.mi.35.100181.001421.

Gendron, R.L., Paradis, H., Ahmad, R., Kao, K., Boyce, D., Good, W.V., Kumar, S., Vasquez, I., Cao, T., Hossain, A., Chakraborty, S., Valderrama, K., Santander, J., 2020. CD10+ cells and IgM in pathogen response in lumpfish (*Cyclopterus lumpus*) eye tissues. Front. Immunol. 11, 1–18. https://doi.org/10.3389/fimmu.2020.576897.

Gnanagobal, H., Cao, T., Hossain, A., Dang, M., Hall, J.R., Kumar, S., Van Cuong, D., Boyce, D., Santander, J., 2021. Lumpfish (*Cyclopterus lumpus*) is susceptible to *Renibacterium salmoninarum* infection and induces cell-mediated immunity in the chronic stage. Front. Immunol.

Gnanagobal, H., Santander, J., 2022. Host-pathogen interactions of marine gram-positive bacteria. Biology 11. https://doi.org/10.3390/biology11091316.

Grinde, B., Lie, Ø., Poppe, T., Salte, R., 1988. Species and individual variation in lysozyme activity in fish of interest in aquaculture. Aquaculture 68, 299–304.

Haugland, G.T., Jakobsen, R.A., Vestvik, N., Ulven, K., Stokka, L., Wergeland, H.I., 2012. Phagocytosis and respiratory burst activity in lumpsucker (*Cyclopterus lumpus* L.) leucocytes analysed by flow cytometry. PLoS One 7, e47909. https://doi.org/10.1371/journal.pone.0047909.

Hood, M.I., Skaar, E.P., 2012. Nutritional immunity: transition metals at the pathogen-host interface. Nat. Rev. Microbiol. 10, 525–537. https://doi.org/10.1038/nrmicro2836.

Imsland, A.K., Reynolds, P., Eliassen, G., Hangstad, T.A., Foss, A., Vikingstad, E., Elvegård, T.A., 2014. The use of lumpfish (*Cyclopterus lumpus* L.) to control sea lice (*Lepeophtheirus salmonis* Krøyer) infestations in intensively farmed Atlantic salmon (Salmo salar L.). Aquaculture 424–425, 18–23. https://doi.org/10.1016/j.aquaculture.2013.12.033.

Imsland, A.K.D., Hanssen, A., Nytrø, A.V., Reynolds, P., Jonassen, T.M., Hangstad, T.A., Elvegård, T.A., Urskog, T.C., Mikalsen, B., 2018. It works! Lumpfish can significantly lower sea lice infestation in large-scale salmon farming. Biol. Open 7, 1–6. https://doi.org/10.1242/bio.036301.

Janeway, C.A., Medzhitov, R., 2002. Innate immune recognition. Annu. Rev. Immunol. 20, 197–216. https://doi.org/10.1146/annurev.immunol.20.083001.084359.

Jansson, E., Ljungberg, O., 1998. Detection of humoral antibodies to *Renibacterium salmoninarum* in rainbow trout *Oncorhynchus mykiss* and Atlantic salmon *Salmo salar* challenged by immersion and in naturally infected populations. Dis. Aquat. Org. 33, 93–99.

Kaattari, S.L., Piganelli, J.D., 1997. Immunization with bacterial antigens: bacterial kidney disease. Dev. Biol. Stand. 90, 145–152.

Kang, D., Liu, G., Lundström, A., Gelius, E., Steiner, H., 1998. A peptidoglycan recognition protein in innate immunity conserved from insects to humans. Proc. Natl. Acad. Sci. U.S.A. 95, 10078–10082. https://doi.org/10.1073/pnas.95.17.10078.

Kim, M.Y., Jang, J.H., Lee, J.-W., Cho, J.H., 2010. Molecular cloning and characterization of peptidoglycan recognition proteins from the rockfish, Sebastes schlegeli. Fish Shellfish Immunol. 28, 632–639. https://doi.org/10.1016/j.fsi.2009.12.023.

Kono, T., Sakai, T., Sakai, M., 2003. Molecular cloning and expression analysis of a novel caspase recruitment domain protein (CARD) in common carp *Cyprinus carpio* L. Gene 309, 57–64. https://doi.org/10.1016/S0378-1119(03)00494-3.

Kukurba, K.R., Montgomery, S.B., 2015. RNA sequencing and analysis. Cold Spring Harb. Protoc. 2015, 951–969. https://doi.org/10.1101/pdb.top084970.

Lauth, X., Babon, J.J., Stannard, J.A., Singh, S., Nizet, V., Carlberg, J.M., Ostland, V.E., Pennington, M.W., Norton, R.S., Westerman, M.E., 2005. Bass hepcidin synthesis, solution structure, antimicrobial activities and synergism, and in vivo hepatic

response to bacterial infections. J. Biol. Chem. 280, 9272–9282. https://doi.org/10.1074/jbc.M411154200.
Li, B., Ruotti, V., Stewart, R.M., Thomson, J.A., Dewey, C.N., 2010. RNA-Seq gene expression estimation with read mapping uncertainty. Bioinformatics 26, 493–500. https://doi.org/10.1093/bioinformatics/btp692.
Li, X., Wang, S., Qi, J., Echtenkamp, S.F., Chatterjee, R., Wang, M., Boons, G.-J., Dziarski, R., Gupta, D., 2007. Zebrafish peptidoglycan recognition proteins are bactericidal amidases essential for defense against bacterial infections. Immunity 27, 518–529. https://doi.org/10.1016/j.immuni.2007.07.020.
Liu, F., Su, B., Fu, Q., Shang, M., Gao, C., Tan, F., Li, C., 2017. Identification, characterization and expression analysis of TLR5 in the mucosal tissues of turbot (*Scophthalmus maximus* L.) following bacterial challenge. Fish Shellfish Immunol. 68, 272–279. https://doi.org/10.1016/j.fsi.2017.07.021.
Lokau, J., Schoeder, V., Haybaeck, J., Garbers, C., 2019. Jak-stat signaling induced by interleukin-6 family cytokines in hepatocellular carcinoma. Cancers 11. https://doi.org/10.3390/cancers11111704.
Lucas, P.C., Yonezumi, M., Inohara, N., McAllister-Lucas, L.M., Abazeed, M.E., Chen, F. F., Yamaoka, S., Seto, M., Núñez, G., 2001. Bcl10 and MALT1, independent targets of chromosomal translocation in MALT lymphoma, cooperate in a novel NF-κB signaling pathway. J. Biol. Chem. 276, 19012–19019. https://doi.org/10.1074/jbc.M009984200.
Makrinos, D.L., Bowden, T.J., 2016. Natural environmental impacts on teleost immune function. Fish Shellfish Immunol. 53, 50–57. https://doi.org/10.1016/j.fsi.2016.03.008.
Miller, L.K., 1997. Baculovirus interaction with host apoptotic pathways. J. Cell. Physiol. 173, 178–182.
Munang'andu, H., 2018. Intracellular bacterial infections: a challenge for developing cellular mediated immunity vaccines for farmed fish. Microorganisms 6, 33. https://doi.org/10.3390/microorganisms6020033.
Nakao, M., Tsujikura, M., Ichiki, S., Vo, T.K., Somamoto, T., 2011. The complement system in teleost fish: progress of post-homolog-hunting researches. Dev. Comp. Immunol. 35, 1296–1308. https://doi.org/10.1016/j.dci.2011.03.003.
Nemeth, E., Ganz, T., 2006. Regulation of iron metabolism by hepcidin. Annu. Rev. Nutr. 26, 323–342.
Neves, J.V., Ramos, M.F., Moreira, A.C., Silva, T., Gomes, M.S., Rodrigues, P.N.S., 2017. Hamp1 but not Hamp2 regulates ferroportin in fish with two functionally distinct hepcidin types. Sci. Rep. 7, 1–14.
Ng, A., Heynen, M., Luensmann, D., Subbaraman, L.N., Jones, L., 2013. Optimization of a fluorescence-based lysozyme activity assay for contact lens studies. Curr. Eye Res. 38, 252–259. https://doi.org/10.3109/02713683.2012.757324.
Pascho, R.J., Elliott, D.G., Chase, D.M., 2002. Comparison of Traditional and Molecular Methods for Detection of *Renibacterium Salmoninarum*, pp. 157–209. https://doi.org/10.1007/978-94-017-2315-2_7.
Pereira, M.B., Wallroth, M., Jonsson, V., Kristiansson, E., 2018. Comparison of normalization methods for the analysis of metagenomic gene abundance data. BMC Genom. 19, 274. https://doi.org/10.1186/s12864-018-4637-6.
Pietretti, D., Wiegertjes, G.F., 2014. Ligand specificities of Toll-like receptors in fish: indications from infection studies. Dev. Comp. Immunol. 43, 205–222. https://doi.org/10.1016/j.dci.2013.08.010.
Powell, A., Treasurer, J.W., Pooley, C.L., Keay, A.J., Lloyd, R., Imsland, A.K., Garcia de Leaniz, C., 2018. Use of lumpfish for sea-lice control in salmon farming: challenges and opportunities. Rev. Aquacult. 10, 683–702.
Rimstad, E., Basic, D., Gulla, S., Hjeltnes, B., Mortensen, S., 2017. Risk assessment of fish health associated with the use of cleaner fish in aquaculture. Opin. panel Anim. Heal. Welf. Nor. Sci. Comm. Food Environ. VKM Rep. 32.
Robinson, M.D., McCarthy, D.J., Smyth, G.K., 2010. edgeR: a Bioconductor package for differential expression analysis of digital gene expression data. Bioinformatics 26, 139–140. https://doi.org/10.1093/bioinformatics/btp616.
Rømer Villumsen, K., Dalsgaard, I., Holten-Andersen, L., Raida, M.K., 2012. Potential role of specific antibodies as important vaccine induced protective mechanism against *Aeromonas salmonicida* in rainbow trout. PLoS One 7, e46733. https://doi.org/10.1371/journal.pone.0046733.
Rønneseth, A., Ghebretnsae, D.B., Wergeland, H.I., Haugland, G.T., 2015. Functional characterization of IgM+ B cells and adaptive immunity in lumpfish (*Cyclopterus lumpus* L.). Dev. Comp. Immunol. 52, 132–143. https://doi.org/10.1016/j.dci.2015.05.010.
Rønneseth, A., Haugland, G.T., Colquhoun, D.J., Brudal, E., Wergeland, H.I., 2017. Protection and antibody reactivity following vaccination of lumpfish (*Cyclopterus lumpus* L.) against atypical *Aeromonas salmonicida*. Fish Shellfish Immunol. 64, 383–391. https://doi.org/10.1016/j.fsi.2017.03.040.
Rose, A.S., Levine, R.P., 1992. Complement-mediated opsonisation and phagocytosis of *Renibacterium salmoninarum*. Fish Shellfish Immunol. 2, 223–240. https://doi.org/10.1016/S1050-4648(05)80061-0.
Rozas-Serri, M., Lobos, C., Correa, R., Ildefonso, R., Vásquez, J., Muñoz, A., Maldonado, L., Jaramillo, V., Coñuecar, D., Oyarzún, C., 2020. Atlantic salmon pre-smolt survivors of *Renibacterium salmoninarum* infection show inhibited cell-mediated adaptive immune response and a higher risk of death during the late stage of infection at lower water temperatures. Front. Immunol. 11, 1378.
Sambrook and Russel, 2001. Molecular Cloning: a Laboratory Manual, second ed. Cold Spring Harbor Laboratory Press, New York.
Sanders, J.E., Fryer, J.L., 1980. *Renibacterium salmoninarum* gen. nov., sp. nov., the causative agent of bacterial kidney disease in salmonid fishes. Int. J. Syst. Evol. Microbiol. 30, 496–502.
Saurabh, S., Sahoo, P.K., 2008. Lysozyme: an important defence molecule of fish innate immune system. Aquacult. Res. 39, 223–239.
Seif, F., Khoshmirsafa, M., Aazami, H., Mohsenzadegan, M., Sedighi, G., Bahar, M., 2017. The role of JAK-STAT signaling pathway and its regulators in the fate of T helper cells. Cell Commun. Signal. 15, 1–13. https://doi.org/10.1186/s12964-017-0177-y.
Shannon, P., Markiel, A., Ozier, O., Baliga, N.S., Wang, J.T., Ramage, D., Amin, N., Schwikowski, B., Ideker, T., 2003. Cytoscape: a software environment for integrated models of biomolecular interaction networks. Genome Res. 13, 2498–2504. https://doi.org/10.1101/gr.1239303.
Siwicki, A., Studnicka, M., 1987. The phagocytic ability of neutrophils and serum lysozyme activity in experimentally infected carp, Cyprinus carpio L. J. Fish. Biol. 31, 57–60.
Sudhagar, A., Kumar, G., El-Matbouli, M., 2018. Transcriptome analysis based on RNA-seq in understanding pathogenic mechanisms of diseases and the immune system of fish: a comprehensive review. Int. J. Mol. Sci. 19, 245. https://doi.org/10.3390/ijms19010245.
Teng, M., Love, M.I., Davis, C.A., Djebali, S., Dobin, A., Graveley, B.R., Li, S., Mason, C. E., Olson, S., Pervouchine, D., Sloan, C.A., Wei, X., Zhan, L., Irizarry, R.A., 2016. Erratum to: a benchmark for RNA-seq quantification pipelines. Genome Biol. 17, 203. https://doi.org/10.1186/s13059-016-1060-7.
Tsujita, T., Tsukada, H., Nakao, M., Oshiumi, H., Matsumoto, M., Seya, T., 2004. Sensing bacterial flagellin by membrane and soluble orthologs of toll-like receptor 5 in rainbow trout (*Onchorhynchus mykiss*). J. Biol. Chem. 279, 48588–48597. https://doi.org/10.1074/jbc.M407634200.
Turaga, P., Wiens, G., Kaattari, S., 1987. Bacterial kidney disease: the potential role of soluble protein antigen(s). J. Fish. Biol. 31, 191–194. https://doi.org/10.1111/j.1095-8649.1987.tb05312.x.
Uribe, C., Folch, H., Enríquez, R., Moran, G., 2011. Innate and adaptive immunity in teleost fish: a review. Vet. Med. 56, 486.
Valenzuela-Miranda, D., Gallardo-Escárate, C., 2018. Dual RNA-Seq uncovers metabolic amino acids dependency of the intracellular bacterium *Piscirickettsia salmonis* infecting Atlantic salmon. Front. Microbiol. 9, 2877.
Wiens, G.D., 2011. Bacterial kidney disease (*Renibacterium salmoninarum*). In: Woo, P.T. K., Bruno, D.W. (Eds.), FIsh Diseases and Disorders. CABI, Wallingford, UK, pp. 338–374.
Wiens, G.D., Rockey, D.D., Wu, Z., Chang, J., Levy, R., Crane, S., Chen, D.S., Capri, G.R., Burnett, J.R., Sudheesh, P.S., Schipma, M.J., Burd, H., Bhattacharyya, A., Rhodes, L. D., Kaul, R., Strom, M.S., 2008. Genome sequence of the fish pathogen *Renibacterium salmoninarum* suggests reductive evolution away from an environmental *Arthrobacter* ancestor. J. Bacteriol. 190, 6970–6982. https://doi.org/10.1128/JB.00721-08.
Xue, X., Caballero-Solares, A., Hall, J.R., Umasuthan, N., Kumar, S., Jakob, E., Skugor, S., Hawes, C., Santander, J., Taylor, R.G., Rise, M.L., 2021. Transcriptome profiling of atlantic salmon (*Salmo salar*) parr with higher and lower pathogen loads following *Piscirickettsia salmonis* infection. Front. Immunol. 12, 789465 https://doi.org/10.3389/fimmu.2021.789465.
Zhang, L., Gao, C., Liu, F., Song, L., Su, B., Li, C., 2016. Characterization and expression analysis of a peptidoglycan recognition protein gene, SmPGRP2 in mucosal tissues of turbot (*Scophthalmus maximus* L.) following bacterial challenge. Fish Shellfish Immunol. 56, 367–373. https://doi.org/10.1016/j.fsi.2016.07.029.